Nano Research Energy

ISSN 2791-0091 (print); 2790-8119 (online)
https://doi.org/10.26599/NRE.2024.9120138

Review Article

Advances and prospects of g-C_3N_4 in lithium-sulfur batteries

Hong Yin[1,2] (✉), Jin He[1], Bo Xiao[1], Miao Zhou[1], Wei Wang[1], Joao Cunha[2], Zuxin Chen[3], Zhaohui Hou[1], Tianqi Zhang[2,4] (✉), and Zhipeng Yu[2] (✉)

[1] *School of Chemistry and Chemical Engineering, Key Laboratory of Hunan Province for Advanced Carbon-based Functional Materials, Hunan Institute of Science and Technology, Yueyang 414006, China*
[2] *International Iberian Nanotechnology Laboratory (INL), Av. Mestre Jose Veiga, 4715-330 Braga, Portugal*
[3] *School of Semiconductor Science and Technology, South China Normal University, Foshan 528225, China*
[4] *Key Laboratory of Marine Chemistry Theory and Technology (Ocean University of China), Ministry of Education, Qingdao 266100, China*

Received: 8 July 2024 / **Revised:** 18 August 2024 / **Accepted:** 30 August 2024

ABSTRACT

Lithium-sulfur (Li-S) batteries are regarded as one of the most promising candidates for next-generation high-energy-density storage systems due to their superior energy density, cost-effectiveness, and environmental friendliness. However, several critical challenges impede their practical application, including the shuttle effect, low conductivity, and volume expansion. Graphitic carbon nitride (g-C_3N_4), with its unique structure and properties, offers potential advantages in catalysis, polarization inhibition, electron conductivity, and sulfurization resistance, which may address these issues. This review concentrates on applying g-C_3N_4 material to enhance Li-S battery performance. The research progress on g-C_3N_4 in this context is explored from two primary perspectives: the modification of g-C_3N_4 itself and its compounding with other materials. Regarding the modification of g-C_3N_4, the focus is on defect engineering and the nanocrystallization of its structure. In terms of composites, the review examines the use of g-C_3N_4 doped with metals, non-metals, graphene, porous carbon, and heterojunctions in electrodes and electrolytes. Ultimately, this review proposes strategies for the rational design of g-C_3N_4 materials to optimize their application in Li-S batteries. Reviewing the current research progress and trends aims to provide new insights and directions for future research in the field.

KEYWORDS

graphitic carbon nitride, defect engineering, heteroatom doping, rational design, lithium-sulfur batteries

1 Introduction

Against national imperatives, the advancement of lithium-sulfur (Li-S) battery technology holds paramount strategic importance. It can address the escalating requirements for energy storage and offers high energy density solutions for electric vehicles, renewable energy sources, and portable electronic devices. Concurrently, the robust growth of the Li-S battery sector will catalyze the enhancement of associated industrial chains, foster job creation, and spur economic prosperity. Moreover, adopting Li-S batteries can diminish reliance on imported lithium resources, fortify national energy security, and contribute to mitigating climate change by curbing greenhouse gas emissions. Thus, the Li-S battery technology is a prominent option for a clean, sustainable, secure, and efficient energy storage system. Notably, Li-S batteries exhibit exceptionally high theoretical specific energy density (2600 Wh·kg^{-1}) and specific capacity (1675 mAh·g^{-1}) [1, 2], positioning them as promising contenders for the forthcoming era of high energy density storage solutions. The practical application of Li-S batteries is impeded by challenges such as the dissolution of cathode material, lithium dendrite formation [3, 4], shuttle effect [5, 6], and volume expansion [7, 8]. These obstacles significantly constrain the energy density of Li-S batteries, falling short of their theoretical potential. As a result, commercialization of this technology remains challenging. In a groundbreaking development in 2009, Ji et al. [9] pioneered using mesoporous carbon and elemental sulfur mixtures, laying the foundation for carbon-coated sulfur materials. Subsequent advancements, including functionalizing carbon materials such as nano-graphene, porous carbon materials, carbon nanoparticles, and carbon nanofibers, have significantly enhanced the electrochemical performance of Li-S batteries [10–13] and partially addressed existing challenges. Researchers have continued to explore innovative doping composite methods, incorporating metal, non-metal, heterojunction, co-doping, and other techniques.

In terms of improving Li-S batteries, the scientific research field currently carries out a variety of modifications for cathode materials, including nanocrystallization, carbon encapsulation and chemical modification. Nanostructured electrode materials, such as nanoparticles, nanowires, nanosheets, etc., can improve the

Address correspondence to Hong Yin, Hong.yin@inl.int; Tianqi Zhang, Tianqi.Zhang@inl.int; Zhipeng Yu, Zhipeng.yu@inl.int

cycle stability and electrochemical performance of batteries, increase the specific surface area, shorten the diffusion path, and improve the Li-ion diffusion rate and storage capacity [14, 15]. Carbon encapsulation provides better electronic conductivity and structural stability by wrapping cathode materials with carbon materials (such as carbon nanotubes, graphene), reducing capacity decay and volume expansion, and extending battery life. Chemical modifications regulating the material's electrochemical properties and stability, such as introducing functional groups and doping other elements, can improve electron conductivity, Li-ion diffusion and cycle stability [16, 17]. These modification methods have scientific research value, help to improve the performance and stability of Li-S batteries, and support commercial applications. However, there are still challenges, such as battery cost, scalability and safety, and researchers need to make unremitting efforts to find better ways to modify cathode materials to promote the performance and application prospects of Li-S batteries.

Graphitic carbon nitride ($g\text{-}C_3N_4$), a unique two-dimensional (2D) layered nitrogenous carbon-based material, has shown increasing potential in energy storage due to its advantages of high-cost efficiency, flexible modulation and simple synthesis in recent years [18]. $g\text{-}C_3N_4$ has an appropriate energy gap structure, good photocatalytic performance and high stability, so it can absorb light energy in the visible range, can use light energy to catalyze water decomposition, carbon dioxide reduction, etc., and has good chemical and thermal stability, which is suitable for applications under various environmental conditions. Currently, $g\text{-}C_3N_4$ is predominantly utilized in various fields, including photocatalysis [19], electrocatalysis [20], material science [21], and environmental protection [22]. $g\text{-}C_3N_4$ can also be used as a modifier for cathode materials of Li-S batteries because of its excellent electrocatalytic performance and large specific surface area. $g\text{-}C_3N_4$ can form a composite material with sulfide, improve the cycle stability and rate performance of Li-S batteries, and thus improve the electrochemical performance. Moreover, $g\text{-}C_3N_4$ has a good complexation adsorption effect with polysulfide and other by-products, which can effectively reduce the shuttle effect's influence on the battery's performance. At the same time, due to the high conductivity of $g\text{-}C_3N_4$ material, the transmission rate of lithium ions can be accelerated in Li-S batteries, and the charging and discharging efficiency of batteries can be improved. It can be concluded that $g\text{-}C_3N_4$, as a modifier of cathode materials for Li-S batteries, is significant in improving battery performance, stability and cycle life [23].

There has been considerable research on applying $g\text{-}C_3N_4$ in the cathode of Li-S batteries within the scientific community. However, this body of work has few comprehensive summaries and evaluations. This review aims to fill that gap by summarizing the doping of $g\text{-}C_3N_4$ with metals, non-metals, and heterojunction materials, as well as the synthesis of composite materials, to enhance the performance of $g\text{-}C_3N_4$ in Li-S batteries. It also seeks to develop new synthesis methods for $g\text{-}C_3N_4$ and explore compound and doping strategies involving $g\text{-}C_3N_4$ and other materials. By doing so, the application process of $g\text{-}C_3N_4$ in Li-S batteries can be further optimized, thereby promoting the comprehensive commercialization of this technology [24, 25].

2 Overview of $g\text{-}C_3N_4$

$g\text{-}C_3N_4$ is a non-metallic covalent compound composed of carbon and nitrogen. It has a graphitic structure characterized by a layered arrangement similar to graphene. This unique structure endows $g\text{-}C_3N_4$ with distinctive physical and chemical properties, making it an intriguing material for scientific and industrial applications. Due to these properties, $g\text{-}C_3N_4$ has broad application prospects in various fields, including catalysis, photocatalysis, electronic devices, sensors, and energy storage. Its high chemical stability allows it to withstand harsh conditions, while its excellent photoelectric properties enhance its performance in solar energy conversion and electronic applications (Fig. 1). Furthermore, the tunable bandgap of $g\text{-}C_3N_4$ makes it versatile for different applications, as it can be engineered to meet specific requirements. These attributes contribute to $g\text{-}C_3N_4$'s popularity as a material for extensive research and diverse practical applications.

2.1 Structure and properties of $g\text{-}C_3N_4$

$g\text{-}C_3N_4$, a two-dimensional layered carbonitride resembling graphene, features a distinctive delocalized conjugated structure. This structure comprises an infinite extension of triazine rings (C_3N_3) or triazine rings (C_6N_7) [30], with carbon and nitrogen atoms interconnected by covalent bonds to create a hexagonal lattice. The interlayer spacing of $g\text{-}C_3N_4$ is approximately 0.32 nm, the C-C bond length is 0.132 nm, and the C-N bond length is 0.133 nm. This unique layered architecture confers upon $g\text{-}C_3N_4$ a significant specific surface area and a substantial pore structure, yielding numerous active sites. The aggregation of multiple fundamental units results in the formation of a lamellar pore structure with a pore size of around 3 Å [31]. The lamellar structures are held together by a weak van der Waals force (Fig. 2). As a wide band gap semiconductor with an energy band gap of around 2.7 eV, $g\text{-}C_3N_4$ exhibits high light absorption capabilities within the visible light spectrum, rendering it a promising candidate for photocatalysis and photovoltaic applications.

The performance and stability of Li-S batteries can be enhanced by the working mechanism of $g\text{-}C_3N_4$, which involves catalysis, adsorption, electrical conductivity, and structural stability (Fig. 3). To be more precise, $g\text{-}C_3N_4$ has the ability to catalyze the redox reaction of polysulfides, thereby enhancing the reaction rate and energy efficiency of the battery. Its large specific surface area and rich pore structure facilitate the adsorption of polysulfides, thereby reducing their dissolution and shuttle effect, thereby improving the cycle stability and energy density of the battery. Additionally, its good electronic conductivity allows it to improve electron transport efficiency, reduce internal resistance, and improve power density and energy efficiency (Fig. 3(a)). Furthermore, the battery's structural and chemical stability are further improved by the stable structure and chemical properties of $g\text{-}C_3N_4$, which prolongs the battery's cycle and service life (Fig. 3(b)). While inherently possessing low conductivity, introducing impurity atoms via doping, such as metals [32, 33], non-metals [34, 35] and so forth, can alter the electronic structure and charge carrier concentration of $g\text{-}C_3N_4$. Additionally, the formation of heterostructures by combining $g\text{-}C_3N_4$ with conductive materials like graphene and carbon nanotubes enhances the charge transport properties and adjusts the conductivity of $g\text{-}C_3N_4$. Notably, $g\text{-}C_3N_4$ demonstrates notable chemical stability and maintains high stability in various environments, including acidic, alkaline, and organic solvents. Furthermore, its surface readily lends itself to functionalization, enabling the introduction of diverse functional groups through chemical modifications to fine-tune its surface properties and functionalities. Therefore, as a non-metallic photocatalyst, $g\text{-}C_3N_4$ exhibits tremendous potential for addressing environmental pollution and energy shortages due to its unique optical properties, cost-effectiveness, and accessibility [36, 37].

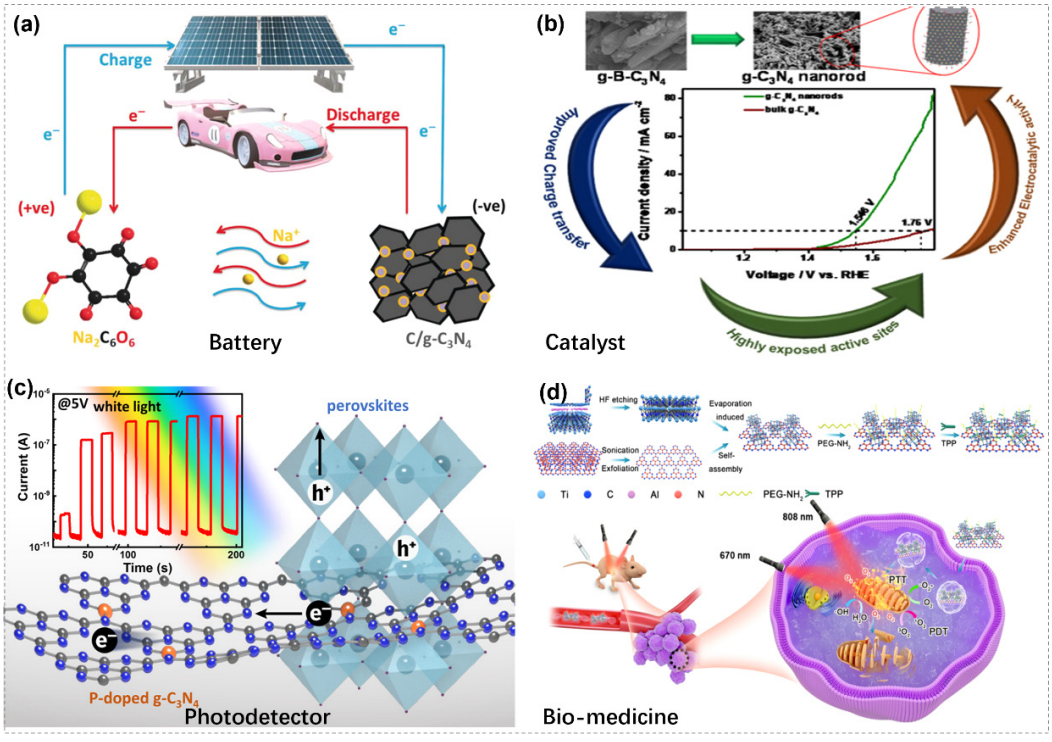

Figure 1 Illustrates the applications of g-C_3N_4 in the fields of battery (a), reproduced with permission from Ref. [26], © Wiley-VCH Verlag GmbH & Co. KGaA, Weinheim 2019. Catalyst (b), reproduced with permission from Ref. [27], © Wiley-VCH Verlag GmbH & Co. KGaA, Weinheim 2019. Photodetector (c), reproduced with permission from Ref. [28], © American Chemical Society 2019. Bio-medicine (d), reproduced with permission from Ref. [29], © American Chemical Society 2024.

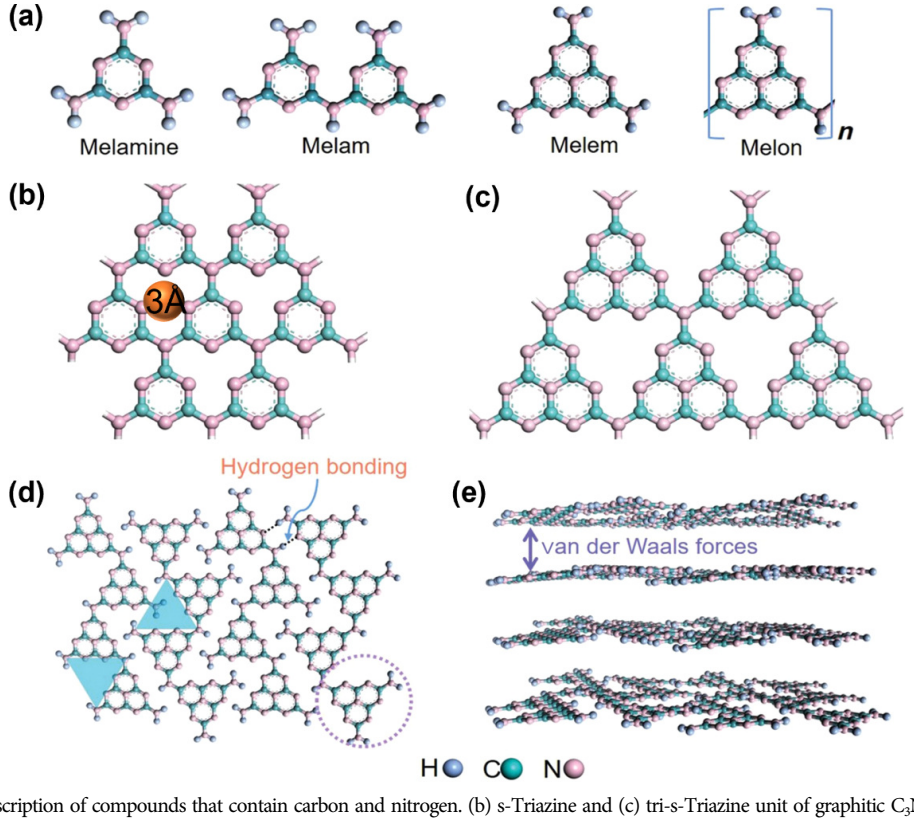

Figure 2 (a) Liebig's description of compounds that contain carbon and nitrogen. (b) s-Triazine and (c) tri-s-Triazine unit of graphitic C_3N_4. (d) Intraplane repeats and (e) the π–π stacking motifs of polymeric carbon nitride. Reproduced with permission from Ref. [31], © Wiley-VCH GmbH 2021.

2.2 Preparation and application of g-C_3N_4

g-C_3N_4 is a two-dimensional material with excellent optoelectronic properties and chemical stability. It has important applications in photocatalysis, optoelectronic devices, sensors, energy storage and other fields. For example, in the field of photocatalysis, g-C_3N_4 can be used as a photocatalyst, using visible light to photolysis water to produce hydrogen or photocatalytic degradation of organic

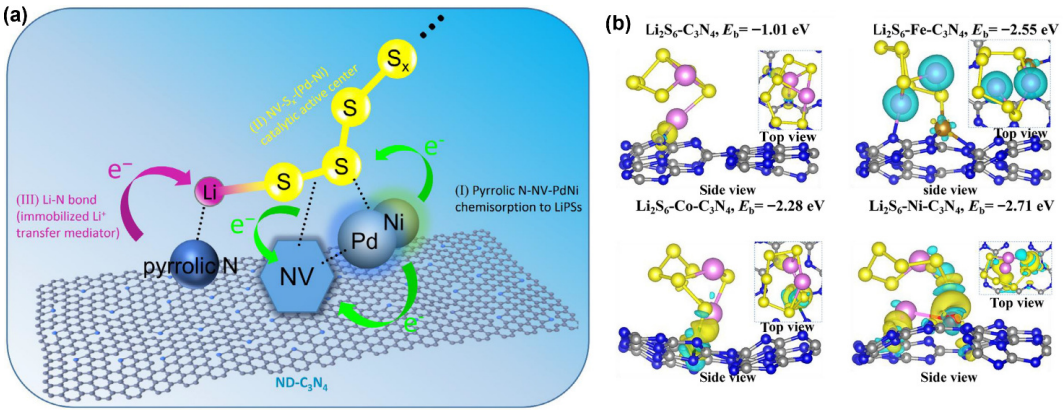

Figure 3 Typical dual mechanisms of g-C_3N_4 in lithium-sulfur batteries. (a) The catalytic mechanism model schematic illustration caused by the cooperative catalytic interface between PdNi@ND-C_3N_4 and LiPSs. Reproduced with permission from Ref. [38], © Elsevier B.V. 2021. (b) The charge density difference of the Li_2S_6. Reproduced with permission from Ref. [39], © Elsevier B.V. 2024.

pollutants. Regarding optoelectronic devices, g-C_3N_4 can be used to fabricate photodiodes, photovoltaic cells, photoelectric triggers and other devices. In addition, g-C_3N_4 can also be used in gas sensors, photocatalytic cells, and other fields. With the in-depth study of the properties and preparation methods of g-C_3N_4, its application prospect will be further expanded and will play an essential role in the field of environmental governance and energy g-C_3N_4 has emerged as a prominent polymer owing to its impressive surface area, and exceptional chemical properties, remarkable thermal stability, and electrical conductivity. Various methods can be employed to obtain g-C_3N_4 structures, including physical [40] or chemical vapor deposition [41, 42], solvothermal synthesis [43, 44], solid-state reactions, and thermal nitriding. Among these, the thermal condensation of cost-effective nitrogen-rich precursors is considered the simplest and most widely utilized method. The thermal condensation of g-C_3N_4 from different precursors like melamine [45, 46], dicyandiamide [47], urea [48], and thiourea [49]. Researchers have explored diverse raw materials and techniques to enhance the quality of g-C_3N_4 for mitigating the shuttle effect in Li-S battery applications.

Jia et al. [50] achieved the synthesis of g-C_3N_4 from trithiocyanuric acid (TTCA) via TTCA polycondensation, resulting in a high n-doping rate of up to 56.87%. The g-C_3N_4-based Li-S batteries exhibit a notable discharge capacity of 1200 mAh·g^{-1} at 0.2 C, with a sustained discharge capacity exceeding 800 mAh·g^{-1} after 100 cycles and a Coulomb efficiency exceeding 99.5%. Huangfu et al. [51] utilized vacuum filtration technology to incorporate an ultra-thin g-C_3N_4 film onto a commercial polypropylene (PP) separator (referred to as g-C_3N_4 separator), effectively restricting polysulfide movement without increasing the overall battery weight. This approach maintains an exceptional convertible capacity of 829 mAh·g^{-1} even after 200 cycles, outperforming traditional PP diaphragm batteries. Employing nanotechnology in g-C_3N_4 production significantly enhances sulfur fixation. Furthermore, Luo et al. [52] developed Co-doped g-C_3N_4 (Co-CN) nanowires through a calcination process. The Co-CN-modified separator demonstrates outstanding stability (achieving 640 mAh·g^{-1} after 250 cycles) and a Coulomb efficiency exceeding 98%. Even with a sulfur mass of 3 mg·cm^{-2}, the battery retains a discharge capacity of 719 mAh·g^{-1} after 100 cycles, exhibiting a capacity retention rate of 95%. The enhanced adsorption and catalytic conversion of polysulfides by the Co-CN nano-chip modified separator effectively mitigated the polysulfide shuttle. These findings underscore the potential of g-C_3N_4 or g-C_3N_4-based materials prepared through efficient processes to address challenges in Li-S battery applications and enhance their practical performance.

3 Optimization and improvement of g-C_3N_4 internal structure

As a material with a unique structure and properties, g-C_3N_4 has certain advantages in catalysis, polarization inhibition, electron conductivity, and sulfurization resistance, which make up for the shortcomings of Li-S batteries. Therefore, applying g-C_3N_4 material in Li-S batteries will be further optimized in three aspects: defect engineering, heteroatom doping, and composite materials.

3.1 Defect engineering

Defect engineering in g-C_3N_4 involves deliberately introducing or regulating defects in g-C_3N_4 materials to alter their physical, chemical, and electronic properties for specific applications or enhance material characteristics. Li et al. [53] developed a nitrogen-deficient porous g-C_3N_4 material (NDCN) using a straightforward preparation method. NDCN exhibits a distinctive three-dimensional structure with abundant macropores and mesopores, facilitating sulfur loading and promoting ion transport, while its ample active sites demonstrate robust LiPS adsorption capabilities. Leveraging these advantages, the Li-S batteries employing the S@NDCN cathode showcase superior long-term cycle stability compared to the S@CN cathode, surpassing 300 cycles at 1 C with a decrease rate of 0.045%. To enhance the capturing of Li_2S_n, Ma et al. [54] designed a functional intermediary layer between the separator and sulfur cathode of the Li-S battery by integrating nitrogen-deficient graphite nitride carbon (g-C_3N_{4-x}) with carbon nanotubes (CNTs). The defect chemistry within g-C_3N_{4-x} enhances polysulfide's chemical affinity and catalyzes polysulfide reactions. Additionally, the intertwined scaffold-like carbon nanotube networks in the g-C_3N_{4-x}/CNT composites expedite electron transfer processes. Capitalizing on this synergistic effect, the discharge capacity of the g-C_3N_{4-x}/CNT modified diaphragm battery reaches 1128 mAh·g^{-1} at 0.2 C, with a reversible capacity of 774 mAh·g^{-1} after 100 cycles. Customizing and enhancing the properties and applications of g-C_3N_4 materials can improve electron transport and ion diffusion during sulfur intercalation and de-intercalation in Li-S cells, facilitating sulfur fixation and reducing sulfide precipitation and dendrite formation. However, striking a balance between defect introduction and material properties is crucial in defect engineering to prevent excessive defect accumulation.

3.2 Heteroatom doping

Heteroatom doping is a common strategy to change the electronic structure and chemical properties of g-C_3N_4 materials by introducing different atoms or ions to replace the atomic position. As an effective method to change polarity, heteroatom doping has been widely studied in carbon materials [55]. This review will be carried out from metal atom doping and non-metal atom doping.

3.2.1 Metal atom doping

Metal heteroatom doping of g-C_3N_4 involves incorporating metals such as iron, nickel, and cobalt to modify the electronic structure and chemical properties of the material. Lu et al. [56] introduced a supported monatomic material (SAFe@g-C_3N_4) with exceptional catalytic activity to enhance the electrochemical conversion kinetics of Li-S batteries (Fig. 4(a)). The SAFe@g-C_3N_4-based Li-S coin cell exhibits a notable reversible specific capacity of 1379 mAh·g^{-1} at 0.1 C, approaching the theoretical capacity. Even after 200 cycles at 0.2 C, the device retains 90% of its capacity, outperforming Li-S batteries utilizing original g-C_3N_4 and b-Fe@g-C_3N_4 under the same conditions. It also delivers a high-rate capacity of 704 mAh·g^{-1} at 5 C (Fig. 4(h)). This cycle performance is competitive with previous reports using various cathode materials. Chen et al. [57] proposed a separator modification strategy employing Ni-C_3N_4/C to suppress polysulfide shuttle and accelerate polysulfide conversion by coordinating transition metals between g-C_3N_4 and crystalline carbon. The Li-S batteries with the Ni-C_3N_4/C modified separator achieve an output of 999 mAh·g^{-1} at 0.5 A·g^{-1}, maintaining an impressive capacity retention rate of 89.4% after 300 cycles. Even with a high sulfur load of 4.6 mg·cm^{-2} and a low electrolyte/sulfur ratio of 6 μL·mg^{-1}, an initial capacity of 724.6 mAh·g^{-1} is obtained at 1.0 A·g^{-1}. Additionally, Zhang et al. [58] developed a two-dimensional copper-doped graphite nitride carbon (Cu-g-C_3N_4) catalyst as a coating material for LSB separators, enhancing redox kinetics in Li-S batteries applications through effective activation of bidirectional reactions.

3.2.2 Nonmetallic atom doping

Lithium polysulfide's diffusion and shuttle effect present a significant challenge in enhancing the energy density and capacity of Li-S batteries, posing a major obstacle to their commercial viability. To tackle this issue, g-C_3N_4 material alters its electronic structure and chemical properties by doping non-metallic elements like nitrogen, sulfur, oxygen, phosphorus, and boron to enhance Li-S battery performance. To boost sulfur utilization and

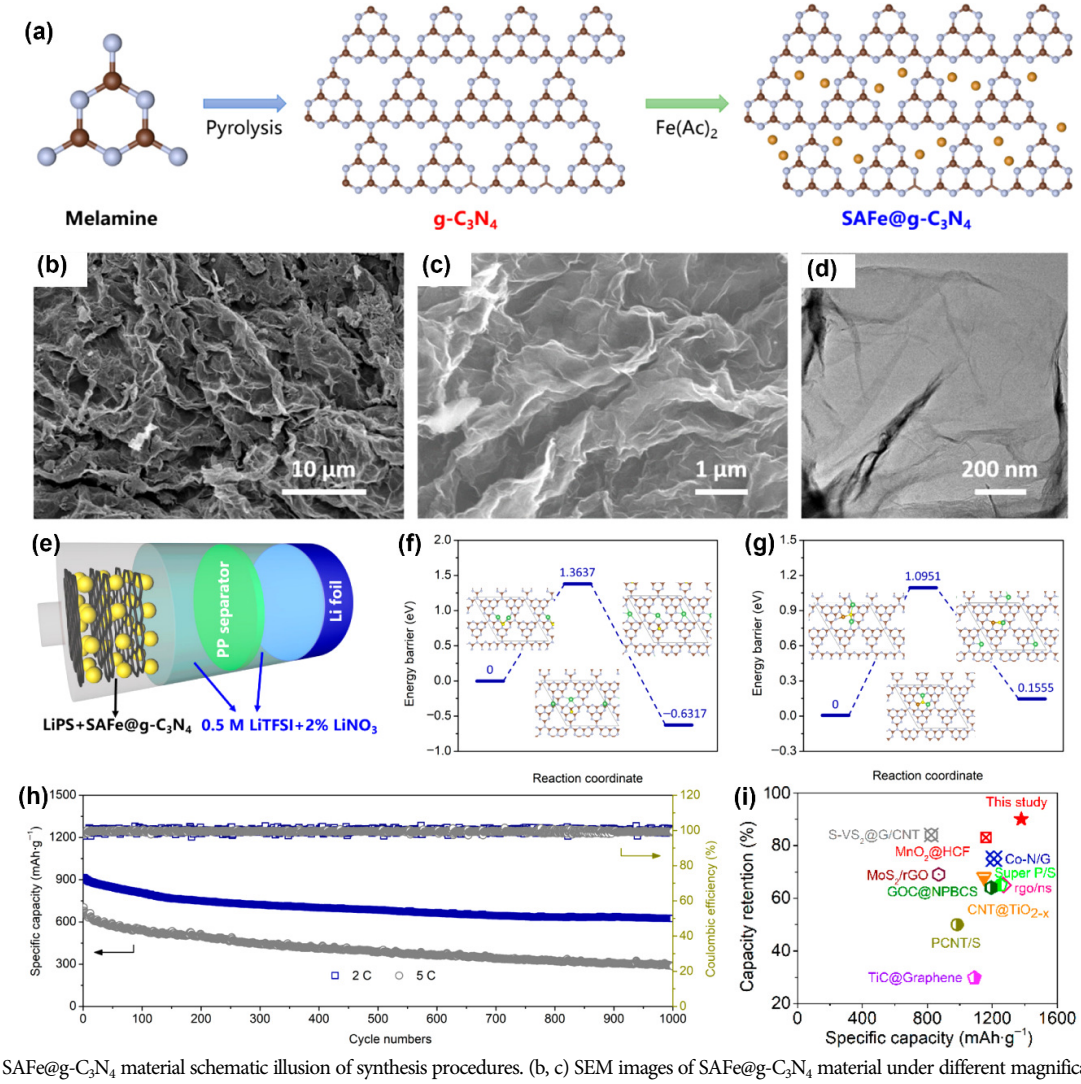

Figure 4 (a) SAFe@g-C_3N_4 material schematic illusion of synthesis procedures. (b, c) SEM images of SAFe@g-C_3N_4 material under different magnifications. (d) TEM images of SAFe@g-C_3N_4 material. (e) Schematic for the structure of battery cell. (f) Li_2S/g-C_3N_4, and (g) Li_2S/SAFe@g-C_3N_4. (h) The long-term stability of the device at current rates of 2 and 5 C. (i) Comparison of specific capacity and capacity retention of Li–S batteries based on various cathode materials. Reproduced with permission from Ref. [56], © American Chemical Society 2020.

capacity retention, Sund et al. [59] integrated a B-doped g-C_3N_4 (BCN) separator into Li-S batteries. The initial specific capacities at 1 C and 2 C are 1050 mAh·g^{-1} and 920 mAh·g^{-1}, respectively, with minimal decay rates of 0.08% and 0.1% after 500 cycles.

Researchers have prepared nanocrystalline non-metallic g-C_3N_4 materials, utilizing larger specific surface areas and enhanced ion/electron transport properties to mitigate shuttle effects and volume changes in Li-S battery applications. Ding et al. [60] introduced oxygen-doped hexagonal tubular carbon nitride (O-TCN) via simple hydrolytic pyrolysis, creating a tubular structure conducive to electrolyte permeation and accommodating sulfur volume changes during redox reactions (Fig. 5(a)). With approximately 80% high pyridine N content as a sulfur host, O-TCN/S facilitates robust capture of polysulfide intermediates through strong N-Li interactions, driving the conversion of high-order polysulfides to low-order Li_2S_2 or Li_2S (Fig. 5(b)). O-TCN displays a first-cycle discharge capacity of 1281 mAh·g^{-1} and sustains a reversible capacity of 401 mAh·g^{-1} after 1000 cycles at 0.5 C, with a cycle decay rate of 0.064% (Figs. 5(c) and 5(d)). Meanwhile, Chen et al. [61] creatively developed the g-C_3N_4 network structure within nitrogen and sulfur co-doped carbonized wood fiber lumen cathode material (NSPCF@CN) using an etching induction strategy for effective polysulfide management and leveraging the advantageous features of the CN network structure-like high specific surface area and unique C-N-C interface-the highly active composites enhanced polysulfide redox kinetics, minimized shuttle effects, and mitigated volume changes during charge-discharge processes. The NSPCF@CN/S electrode demonstrates a remarkable specific capacity of 1590.8 mAh·g^{-1} at 0.5 C, achieving a high rate capacity of 976.9 mAh·g^{-1} at 2.0 C. Impressively, the electrode maintains a high reversible capacity exceeding 781 mAh·g^{-1} after more than 1000 cycles at 1.0 C. Density functional theory (DFT) calculations highlighted the synergistic benefits of N and S co-doping alongside the CN network structure in enhancing polysulfide adsorption capacity, offering a novel approach to resolving complexities associated with Li-S batteries.

The storage, conversion, and transmission processes of lithium sulfide in Li-S batteries can be precisely regulated. Do et al. [62] developed a novel material, carbon and phosphorus nitride (CNP), as an exceptional adsorbent for Li-S batteries. Experimental evidence and DFT computations revealed that CNP exhibits the highest binding energy with Li-S at a 22% phosphorus concentration (CNP22). The interaction of CNP22 with Li-S demonstrated both Li-N bonding and P-S coordination within the sulfur cathode. The introduction of CNP22 into the Li-S system enabled the effective attainment of sufficient charging capacity at a low cutoff voltage (2.45 V), thereby minimizing side effects and extending the cycle life of the Li-S system. After 700 cycles, the CNP22 lithium-ion battery showcases a discharge capacity of up to 850 mAh·g^{-1}, with a cycle stability of 0.041% and a decay rate of 0.041%. Incorporating CNP22 into Li-S batteries yields high performance without concerns about the Li-S shuttle phenomenon. While carbon materials enhance electrode conductivity and mitigate the dissolution and diffusion of lithium polysulfide in Li-S systems, employing single non-functional

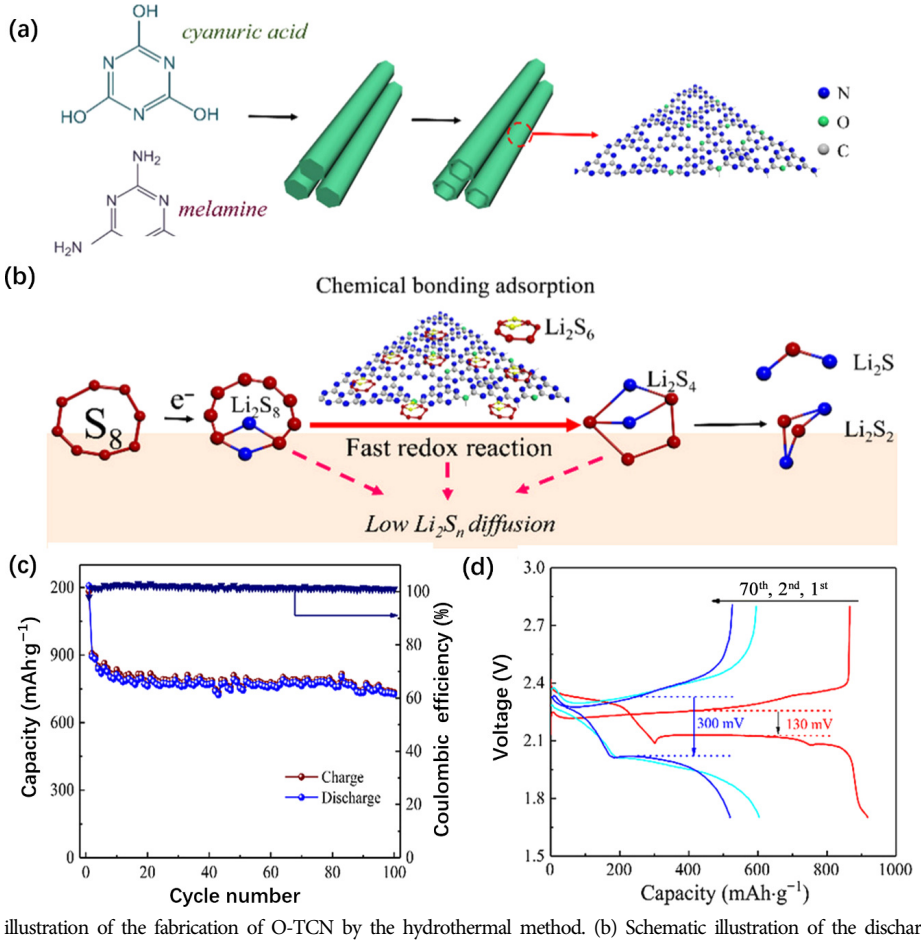

Figure 5 (a) Schematic illustration of the fabrication of O-TCN by the hydrothermal method. (b) Schematic illustration of the discharge process in the sulfur electrode. (c) Galvanostatic charge/discharge voltage profiles O-TCN/S electrodes. (d) Cycling performance O-TCN/S cathode at 0.1 C. Reproduced with permission from Ref. [60], © Ding L., et al. *Energy Technology* published by Wiley-VCH GmbH 2021.

carbon materials directly with sulfur presents limitations. The physical adsorption capacity may be relatively weak, restricting sulfur retention capacity, and the hydrophobic carbon interface could lead to sulfur recombination, hampering the formation of a robust interface with highly polar lithium sulfide. This scenario could impede lithium sulfide precipitation and impact the efficient performance of carbon-sulfur composite electrodes.

3.3 Metal and nonmetal co-doped g-C_3N_4

Metal compound/g-C_3N_4 composites, particularly polar metal compound/g-C_3N_4 composites, have significantly progressed in Li-S battery material modification, interface engineering, and new structure design. One promising approach to limit the diffusion of polysulfides and mitigate the shuttle effect is using metal oxide and carbon composite modified separators. For instance, polar gold compound/g-C_3N_4 composites have been applied to Li-S battery separators. Xu et al. [63] developed a $MoSe_2$@g-C_3N_4 composite material for the interlayer of the separator. The $MoSe_2$@g-C_3N_4 interlayer exhibits an initial capacity 2.2 times higher than conventional polypropylene (PP) separators at 0.5 C. It also demonstrated a low-capacity decay rate of 0.09% after 500 cycles at 0.5 C. At the highest rate of 3 C, the composite material achieves a capacity of 564.2 mAh·g^{-1}. This composite combines the strong adsorption capability of g-C_3N_4 with the appropriate migration of $MoSe_2$ on the surface, offering advantages for Li-S battery applications.

Recently, many scientists have doped metal and non-metal materials together in g-C_3N_4 to improve the performance of Li-S batteries. Wen et al. [64] designed a g-C_3N_4/MoO_3 composite and applied it to modified separators. At a current rate of 4 C, it achieves an initial capacity of 542 mAh·g^{-1} and a capacity decay rate of 0.0053% after 700 cycles. Wang et al. [65] developed a novel dual-function separator for Li-S batteries. The separator consists of a self-assembled FeOOH layer chemically combined with a conductive g-C_3N_4/KB layer through a physical coating. This dual-function separator enables the battery to achieve rate capacities of 1000, 901, and 802 mAh·g^{-1} at 0.5 C, 1 C, and 2 C. Dong et al. [66] developed a functional separator by anchoring polar nano-TiO_2 on the surface of two-dimensional layered g-C_3N_4 and using multi-walled carbon nanotubes as conductive substrates. The modified Li-S battery demonstrates good long-term cycle performance, with an initial specific discharge capacity of 1316 mAh·g^{-1} at 1 C and a high discharge capacity of 569.9 mAh·g^{-1} is maintained after 800 cycles (with a capacity decay rate of only 0.07%). Majumder et al. [67] designed a sulfur carrier using a native polar molybdenum disulfide/g-C_3N_4 porous nanosheet cathode material (MoS_2/g-C_3N_4). The composite exhibits a specific capacity of 430 mAh·g^{-1} after 400 cycles at 8 C, with a low-capacity decay rate of 0.028%. Overall, metallic and non-metallic compound/g-C_3N_4 composites perform well in Li-S battery applications, and the potential to improve battery performance and meet challenges is related to polysulfide diffusion and shuttle effects.

Nanotechnology has played a significant role in improving the application of Li-S batteries. By incorporating various metal compounds, nanotechnology enables the formation of new heterojunctions during the preparation of nano-based g-C_3N_4 materials. The synergistic effect between g-C_3N_4 materials and heterojunctions creates an efficient charge transfer field and effectively mitigates corrosion and aggregation during charge and discharge processes. Xu et al. [68] successfully designed and synthesized a ternary heterojunction of g-C_3N_4/MoS_2/ZnS as a high-performance cathode using a simple one-step hydrothermal method. The presence of g-C_3N_4 and ZnS improved the electrochemical reversibility of MoS_2 in storing Li^+. The electrochemical tests demonstrated that the g-C_3N_4/MoS_2/ZnS electrode exhibits a high reversible capacity and rate capacity, achieving 1310 mAh·g^{-1} at a current density of 0.1 A·g^{-1}. Furthermore, even at 1 A·g^{-1}, the electrode maintained a capacity of 805 mAh·g^{-1}. Li et al. [69] prepared a heterostructure comprising nitrogen-deficient graphite nitride carbon (ND-g-C_3N_4) and MgNCN through thermal denitrification of magnesium. The nitrogen-rich and nitrogen-deficient lithophile g-C_3N_4, combined with thiophile MgNCN, effectively captured lithium polysulfides (LiPSs) and regulated Li_2S nucleation (Fig. 6), bidirectional catalyst with robust lithiophilicity and sulfiphilicity for advanced Li-S battery. The results exhibit excellent electrochemical performance of the Li-S battery with MgNCN/ND-g-C_3N_4 as the intermediate layer, achieving a discharge capacity of 650 mAh·g^{-1} at 4 C, with a capacity decay rate of 0.008% after 400 cycles at 1 C. Even with a sulfur load of 5.1 mg·cm^{-2} (Fig. 6(e)), the battery maintains good capacities at 0.5 C (64.18%) and 1 C (90.46%) as shown in Fig. 6(f), respectively. This strategy presents a new approach for designing high-efficiency catalysts in Li-S batteries.

The provided information describes the efforts of researchers in addressing the shuttle effect of polysulfides in Li-S batteries. Liu et al. [70] successfully prepared Nb_2O_5/g-C_3N_4 composites cathode material through electrospinning and double crucible gas-solid reaction. The composites exhibit improved photocatalytic activity for methylene blue degradation compared to Nb_2O_5 nanofibers and pure g-C_3N_4. The optimized Nb_2O_5/g-C_3N_4 composites also showed promising performance in Li-S batteries, with a high initial discharge capacity of 900 mAh·g^{-1} at 0.5 C and a capacity decay rate below 0.1% after 500 cycles. The study demonstrated the effective adsorption of polysulfides and catalytic conversion of polysulfides by NOCN-8, providing potential applications in environmental remediation and energy fields. In another study by Liu et al. [71] developed a nanocomposite consisting of well-dispersed CoS on g-C_3N_4 nanosheets (CoS@g-C_3N_4). This nanocomposite was integrated into a polypropylene film to form a thin interlayer with a thickness of only 2.1 μm. The interlayer exhibits polysulfide capture through Li-N bonds and Lewis-acid base interactions between CoS and polysulfide anions. Moreover, it catalyzed the redox conversion of intermediate polysulfide. The Li-S battery assembled with the modified separator and high sulfur content cathode demonstrates excellent electrochemical performance, including a specific capacity of 1290 mAh·g^{-1} at 0.2 C and a low attenuation rate of 0.03% after 500 cycles. The study provided insights into the rational design of thin and lightweight interlayers to enhance sulfur utilization and minimize energy density losses and Li-ion transport hindrances in Li-S batteries. These findings contribute to the ongoing efforts to optimize the performance of Li-S batteries and explore potential applications in various fields. It is important to mention that Salman et al. developed a multifunctional cathode material that is based on a three-dimensional MXene and g-C_3N_4 hollow sphere frame [72]. At 0.1 C, a cathode with an 80% sulfur ratio has a primary specific capacity of 1350.6 mAh·g^{-1}. The retention rate is 65.2%, as evidenced by the fact that it retains 877.2 mAh·g^{-1} after 100 cycles. Furthermore, it demonstrates exceptional electrochemical performance in terms of rate performance, with a capacity of 632.5 mAh·g^{-1} at 4 C. The objective of the design is to establish a conductive platform that possesses high absorption and

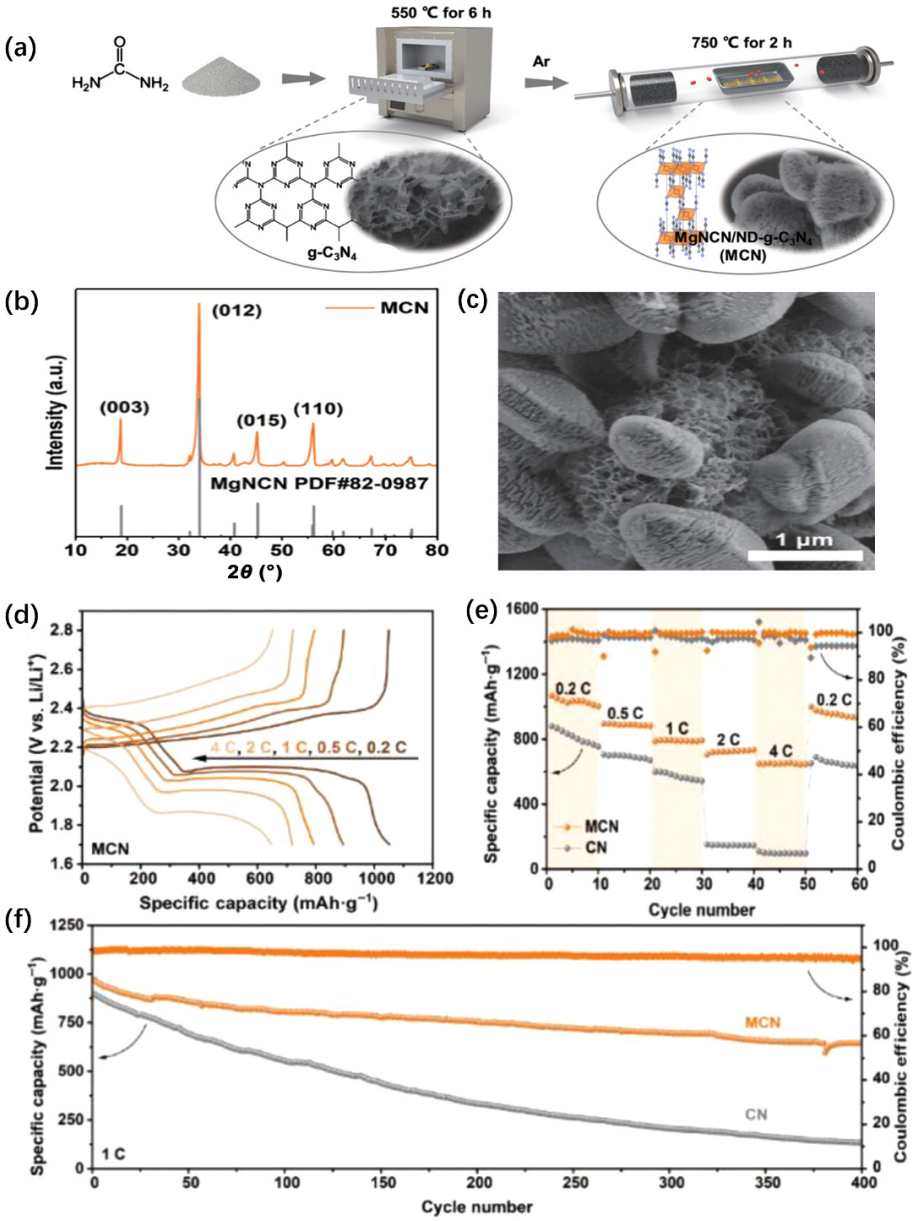

Figure 6 (a) Schematic illustration of the preparation of MCN. (b) XRD patterns. (c) SEM images of MCN material at 10 μm. (d) Galvanostatic charge/discharge voltage profiles of MCN cell at different rates. (e) Rate performance of MCN and CN cells. (f) Cycle performance of MCN and CN cells at 1 C with sulfur loading of 1.2 mg·cm^{-2}. Reproduced with permission from Ref. [69], © Wiley-VCH GmbH 2023.

catalytic capabilities in order to enhance the performance of Li-S cells in real-world operating environments.

4 Design and development of g-C_3N_4 composites

By manipulating the defects in g-C_3N_4 and introducing heteroatom doping to alter its electronic structure and chemical properties, advancements have been made in enhancing the efficiency of Li-S batteries [73, 74]. However, practical observations reveal that sulfides still exhibit dissolution and diffusion issues over extended periods, leading to capacity decay and performance deterioration despite these modifications. Addressing these challenges, this study delves into creating g-C_3N_4 composites using conductive carbon materials, aiming to alleviate significantly, if not entirely resolve, the fundamental obstacles encountered in the practical application of Li-S batteries.

4.1 CNTs conductive network

The conductive network constructed by CNTs offers several advantages in addressing the challenges faced by Li-S batteries [75, 76]. These advantages include enhanced conductive pathways, stable conductivity, improved interface compatibility, and a stable material structure. To achieve nanoscale g-C_3N_4 materials with enhanced properties, researchers have been exploring different preparation materials, methods, optimization conditions, and characterization techniques. Wang et al. [77] proposed a novel method for preparing g-C_3N_4 (PCN)/CNT sulfur carriers through solution precipitation. Protonated g-C_3N_4 (PCN) is uniformly dispersed in H_2SO_4 and self-assembled with CNTs through static electricity. By adjusting the proportion of PCN/CNTs, it has been demonstrated that the PCN/CNTs composite with the optimal ratio of 1:1 (CC1:1) exhibits excellent electrochemical performance. After 500 cycles, the CC1:1/S cathode at 1 C demonstrates a final discharge specific capacity of 711.9 mAh·g^{-1},

with an attenuation rate of only 0.08%. This research highlights the significance of the PCN/CNTs composite in achieving enhanced electrochemical performance and showcases its potential as a promising material for Li-S batteries. In another study by Wang et al., [78] a multifunctional polysulfide barrier reinforced with graphite carbon nitride/carbon nanotube (g-C_3N_4/CNT) composites was developed to impede shuttle behavior and enhance battery performance. The spongy structure of g-C_3N_4, enriched with ion transfer pathways and active interfaces, along with its strong chemical immobilization properties towards lithium polysulfides, played a crucial role in improving the energy density and cycle life of Li-S batteries.

Innovative approaches have further advanced the integration of nano-sized g-C_3N_4 in Li-S batteries. One such study by Zhang et al. [79] involved the fabrication of a g-C_3N_4/carbon heterostructure on graphene nanowires (PCNG) using a phenyl modification strategy and *in-situ* thermal polycondensation. This heterostructure exhibits unique electron cloud distribution, exceptional sulfur immobilization capabilities, and excellent electrical conductivity. The Li-S battery incorporating a simple Samp C cathode and PCNG interlayer demonstrated a high initial capacity of 1192 mAh·g^{-1} at 0.1 C and an impressive cycle life exhibiting a capacity decay rate of only 0.050% after 800 cycles. Moreover, when applied under high sulfur load conditions (7 mg·cm^{-2}), the PCNG/PP separator battery exhibits stable cycling performance. These findings present a novel approach for integrating functionalized g-C_3N_4 in Li-S electrochemistry applications.

The performance and catalytic performance of g-C_3N_4 in Li-S batteries are influenced by its size, as demonstrated by the advantages of the conductive network formed by carbon nanotubes in addressing the issues faced by these batteries [80]. The size of g-C_3N_4 will directly impact its specific surface area and pore structure, thus influencing its ability to adsorb sulfur and its catalytic activity. In general, smaller g-C_3N_4 particles possess a greater specific surface area and a higher number of pores. This characteristic enables them to offer more active sites and sulfur adsorption sites, hence enhancing their catalytic activity. Furthermore, the dimensions of g-C_3N_4 will also have an impact on its electronic configuration and conductivity, thus influencing its catalytic efficiency. Reduced particle size of g-C_3N_4 results in a decreased distance for electron transport and an increased concentration of electrons, leading to improved electron transport efficiency and catalytic activity. Furthermore, the magnitude of g-C_3N_4 will also impact its thermal stability and mechanical properties, thus influencing its long-term stability and cycle performance. Reduced-sized g-C_3N_4 particles have enhanced thermal stability and mechanical strength, hence offering superior long-term stability and cycle performance. In summary, while there may be occasional deviations in certain situations, as a general rule, smaller g-C_3N_4 particles tend to have a favorable influence on the performance of Li-S batteries. Hence, regulating the dimensions of g-C_3N_4 particles can be regarded as a viable approach for enhancing the efficiency of Li-S batteries.

4.2 High conductive graphene

Highly conductive graphene and g-C_3N_4 share similar structures and properties, enabling the effective utilization of highly conductive graphene as a carrier or additive in fabricating g-C_3N_4 composites [81]. A study by Moon et al. [82] employed pyrrole polymerization to coat PPy onto sulfur-loaded g-C_3N_4 and rGO composites (g-C_3N_4/rGO/S@PPy) to develop high-performance cathodes (Fig. 7(a)). The size of as-prepared particles is about 150 nm, showing superior specific surface area (Figs. 7(d) and 7(e)). The g-C_3N_4/rGO/S@PPy composite exhibits a considerable capacity of 1189 mAh·g^{-1} with an impressive retention rate of 91% after 200 cycles, even under a substantial sulfur load of 5 mg·cm^{-2}, demonstrating a high surface capacity of 5.5 mAh·cm^{-2} (Fig. 7(d)). The incorporation of PPy, a conductive polymer, facilitated electron conduction, impeded polysulfide dissolution and enhanced the stability of LSB. This highlights the efficacy of doping g-C_3N_4 into the graphene oxide network with high conductivity to improve the electrochemical performance of Li-S batteries. Song et al. [83] demonstrated control over the structure and morphology of composites by adjusting the initial ratio of g-C_3N_4 to rGO in the hydrothermal reactor. Compared to other composites (CG11, CG51), the g-C_3N_4/rGO sulfur matrix (CG12) exhibits superior performance with higher initial capacity (1146 mAh·g^{-1} at 0.5 C), enhanced magnification (752 mAh·g^{-1} at 1 C, 623 mAh·g^{-1} at 2 C), and stable cycle performance (400 cycles at 1 C). The distinctive hybrid structure of CG12 facilitated optimal interaction between g-C_3N_4 and S_2 molecules, effectively suppressing polysulfide shuttle and enhancing cycle stability. Furthermore, Wang et al. [84] synthesized rGO/g-C_3N_4 and rGO/g-C_3N_4/CNT microspheres through ethanol-assisted spray drying, transforming their structures into regular microspheres. These microspheres provided physical constraints for lithium polysulfide (LiPSs) due to the pores formed by the accumulated rGO, g-C_3N_4, and CNT, supported by the strong chemical adhesion provided by nitrogen atoms enriched by g-C_3N_4. This dual fixation mechanism alleviated the "shuttle effect" in Li-S batteries and contributed to the high cycle stability of the cathode. The discharge capacity of the rGO/g-C_3N_4/CNT/S cathode after 500 cycles reaches 620 mAh·g^{-1}, with a minimal capacity decay rate of 0.03% at 1 C. Notably, the cathode maintained a retained capacity of 712 mAh·g^{-1} after 300 cycles at 0.2 C with a high sulfur load of 4.2 mg·cm^{-2}.

Improvements in sulfur loading and the adsorption/catalysis of lithium polysulfides are essential to optimize carbon-based sulfur cathode for Li-S batteries. Zhao et al. [85] developed rGO/g-C_3N_4 QDs composites on two-dimensional reduced graphene nanowires, offering a novel cathode solution for Li-S batteries (Fig. 8(a)). The incorporation of g-C_3N_4 quantum dots serves a dual purpose by enhancing LiPSs adsorption sites, suppressing the "shuttle effect", and boosting kinetics, while also maintaining high conductivity and a mesoporous structure. This leads to increased sulfur utilization and faster Li^+ charge transfer. Consequently, the S@rGOg-C_3N_4 QDs cathode demonstrated a higher initial discharge capacity of 1013.9 mAh·g^{-1} at 1 C and a better retention capacity of 95.2 mAh·g^{-1} after 500 cycles (0.016% reduction). Notably, it exhibits an excellent area capacity of 16.1 mg·cm^{-2} even under high sulfur loads of 16.2 mA·cm^{-2} (Figs. 8(e)–8(g)) and challenging electrolyte conditions (E_{max}/S ratio is 6.0 μL·mg^{-1}). This study presents an innovative, cost-effective design strategy for high-quality carbon-based sulfur cathodes.

Researchers have explored the introduction of BN (boron nitride) into g-C_3N_4 composites to enhance the performance of Li-S batteries. BN nanowires, one-dimensional honeycomb monolayer ribbon boron nitride materials, exhibit unique electronic properties due to the rotation of P_z orbitals. Many researchers have incorporated BN into g-C_3N_4 composites to improve the Li-S battery's performance. One approach involves coating the cathode surface with a thin BN nanosheet/graphene

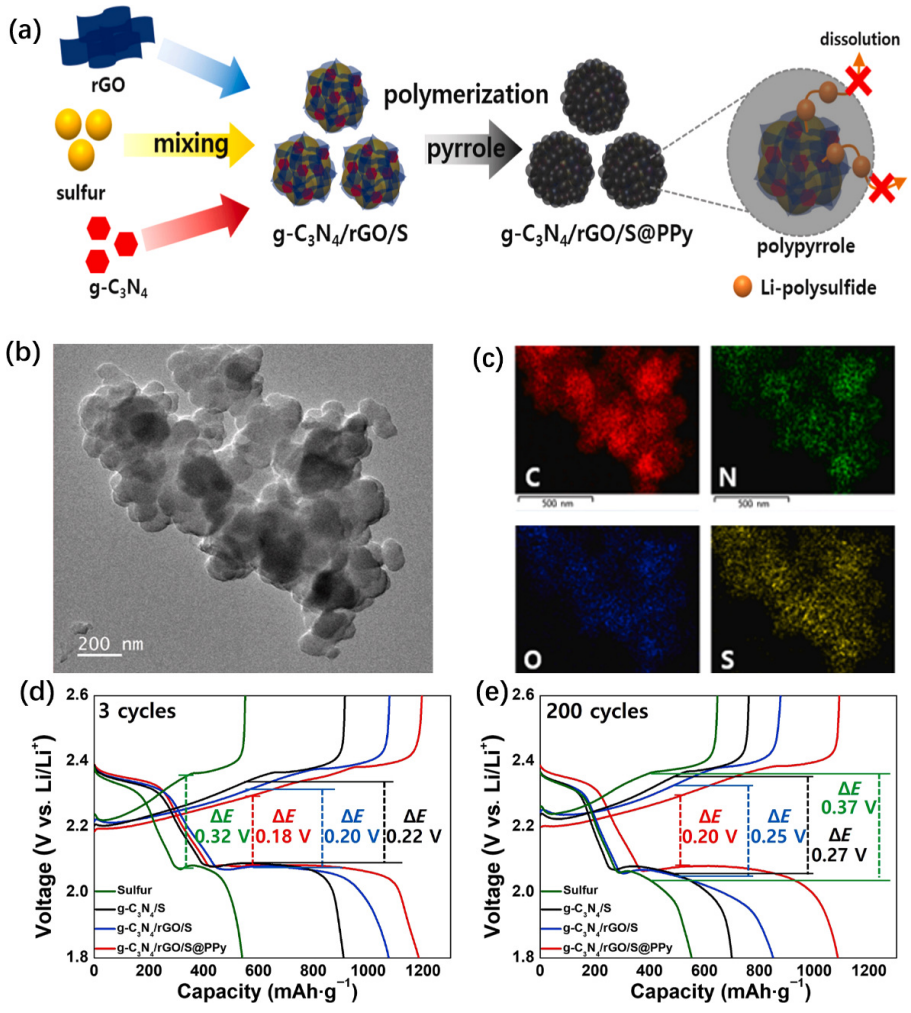

Figure 7 (a) Preparation diagram of g-C_3N_4/rGO/S@PPy. (b) TEM images g-C_3N_4/rGO/S@PPy. (c) EDX images g-C_3N_4/rGO/S@PPy. (d) Cycling performance of sulfur, g-C_3N_4/S, g-C_3N_4/rGO/S, and g-C_3N_4/rGO/S@PPy as the cathodes measured at a current density of 0.2 C for 200 cycles. (e) Charge/discharge curves of the cathode were measured at 200 cycles. Reproduced with permission from Ref. [82], © Elsevier B.V. 2022.

composite film as a protective layer [86, 87]. This coating effectively inhibits the dissolution and diffusion of lithium polysulfide, resulting in significantly improved specific capacity and cycle stability of the sulfur cathode. The capacity decay rate observed during 1000 cycles under 3 C is only 0.0037%. Furthermore, Deng et al. [88] designed a composite ion sieve for Li-S batteries, utilizing a multifunctional intermediate layer of graphite-like carbon nitride (g-C_3N_4), BN, and graphene. Multifunctional ion-sieve constructed by 2D materials as an interlayer for Li-S batteries. The g-C_3N_4 structure contains ordered ion channels with a diameter of 0.3 nm, which effectively block polysulfides while allowing lithium-ion passage. BN serves as a reaction catalyst to facilitate the conversion of polysulfides, while graphene acts as a built-in current collector, providing excellent long-range conductivity. The synergistic effect of these three two-dimensional components enables the battery to cycle reliably for over 500 cycles at a high sulfur load of 6 mg·cm^{-2} and a rate of 1 C.

Introducing ultra-thin 2D graphene into g-C_3N_4 materials aims to enhance their properties further. Graphene, a two-dimensional derivative of graphite, has found widespread applications in various cutting-edge fields of nanoscience and nanotechnology. Wu et al. [89] conducted a study where they prepared a novel renewable n-doped carbonaceous host material (C-NC) through a simple dissolution and carbonization process. This material possesses a three-dimensional network structure and can serve as the sulfur (S) cathode in Li-S batteries (Fig. 9). By incorporating a small amount of graphene (GN) and g-C_3N_4, the resulting composite material, C-NC/GN/g-C_3N_4, maintains the 3D interconnected network structure formed by the assembly of ultra-thin graphene sheets. This composite material offers several advantages. Firstly, the high conductivity of graphene facilitates rapid electron transfer. Secondly, g-C_3N_4 exhibits effective chemical absorption of intermediate polysulfides, inhibiting their detrimental dissolution. Thirdly, the three-dimensional network framework of C-NC, with its high surface area and macro/mesoporous properties, provides a fast ion diffusion pathway and allows for sufficient electrolyte infiltration. This reduces structural changes in the sulfur cathode during cycling. Combining these features, the C-NC/GN/g-C_3N_4 hybrid composite material demonstrates improved performance in Li-S batteries. Based on the provided information, incorporating the S element and employing a cathode structure strategy derived from renewable biomass have significantly enhanced the performance of Li-S batteries. The prepared S@C-NC/GN/g-C_3N_4 cathode exhibits excellent high-rate and remarkable cycle performance. Even after 500 consecutive electrochemical cycles, the reversible capacity of the cathode was maintained at 1130 mAh·g^{-1}. This demonstrates the potential of the cathode structure strategy, which utilizes renewable biomass, as a low-cost and promising approach for designing high-rate and long-life lithium batteries.

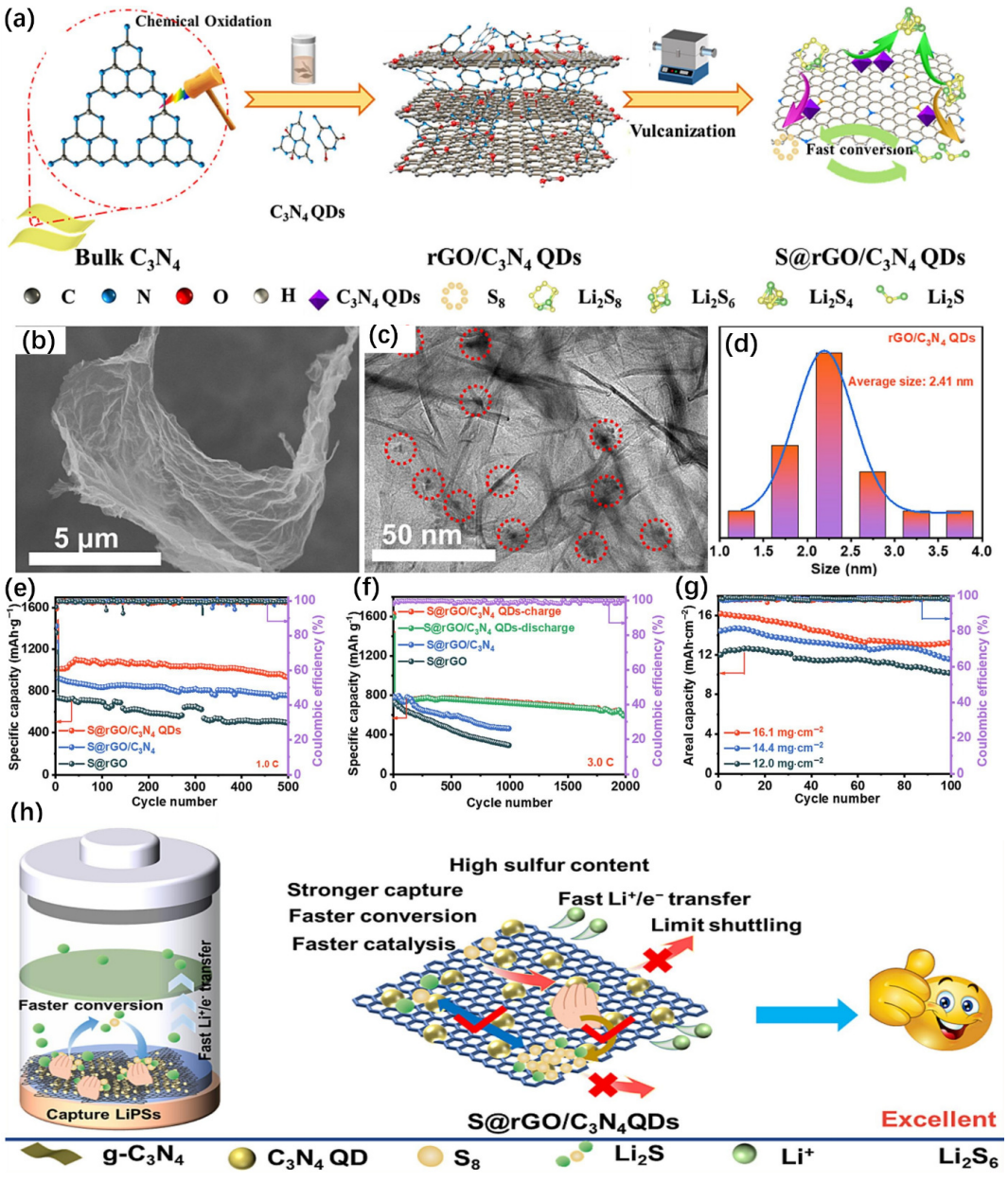

Figure 8 (a) Schematic illustration of the synthesis procedure of rGO/C_3N_4 QDs material. (b) The SEM image, (c) TEM image, (d) particle size distribution. (e) Long-term cycling performances at 1.0 C for different cathodes. (f) Long-term cycling performances at 3.0 C for S@rGO/C_3N_4 QDs cathode. (g) Cycling performances at 0.1 C of S@rGO/C_3N_4 QDs cathode with ultra-high sulfur loading. (h) Schematic illustrating the mechanism of the high-performance LSBs with S@ rGO/C_3N_4 QDs cathode. Reproduced with permission from Ref. [85], © Elsevier B.V. 2023.

The incorporation of a 2D g-C_3N_4/graphene sheet composite (g-C_3N_4/GS as an intermediate layer in the S/KB cathodes has shown promise in addressing the degradation of electrochemical performance caused by the "shuttle effect" of dissolved lithium polysulfide. The g-C_3N_4/GS interlayer, with its laminated structure and physical and chemical interactions, effectively traps polysulfides. The thin g-C_3N_4/GS interlayer significantly suppresses dissolved polysulfides (Li_2S_x: $2<x\leq8$) and enhances the discharge capacity of the S/KB cathode. Compared to using the S/KB cathode alone, the S/KB@g-C_3N_4/GS cathode exhibits a discharge capacity of 1191.7 mAh·g^{-1} at 0.1 C. It maintains a good cycle life with a discharge capacity of up to 612.4 mAh·g^{-1} after 100 cycles [90]. These findings highlight the potential of incorporating S@C-NC/GN/g-C_3N_4 cathodes and g-C_3N_4/GS interlayers in Li-S batteries to improve their performance, overcome the "shuttle effect", and extend their cycle life.

4.3 Porous carbon materials

Porous carbon materials are known for their abundant pores and high surface area, which provide a more significant number of reactive surfaces. Zou et al. [91] conducted a study where they prepared an n-doped porous carbon-coated graphite carbon nitride heterojunction (g-C_3N_4/g-C_3N_4@C) cathode materials by growing a g-C_3N_4/g-C_3N_4 heterojunction on the pores of porous carbon. The effective interfacial adhesion between the g-C_3N_4/g-C_3N_4 heterojunction and the highly conductive porous carbon, acting as a sulfur host, ensured an initial specific capacity of 752 mAh·g^{-1} at 1 C for the Li-S battery. After 400 cycles at 1 C, the reversible capacity was 496 mAh·g^{-1}, and at 2 C, the higher rate capacity reached 468 mAh·g^{-1} after 500 cycles. The enhanced electrochemical performance of this ternary synergistic system is attributed to the effective interfacial adhesion and conductivity

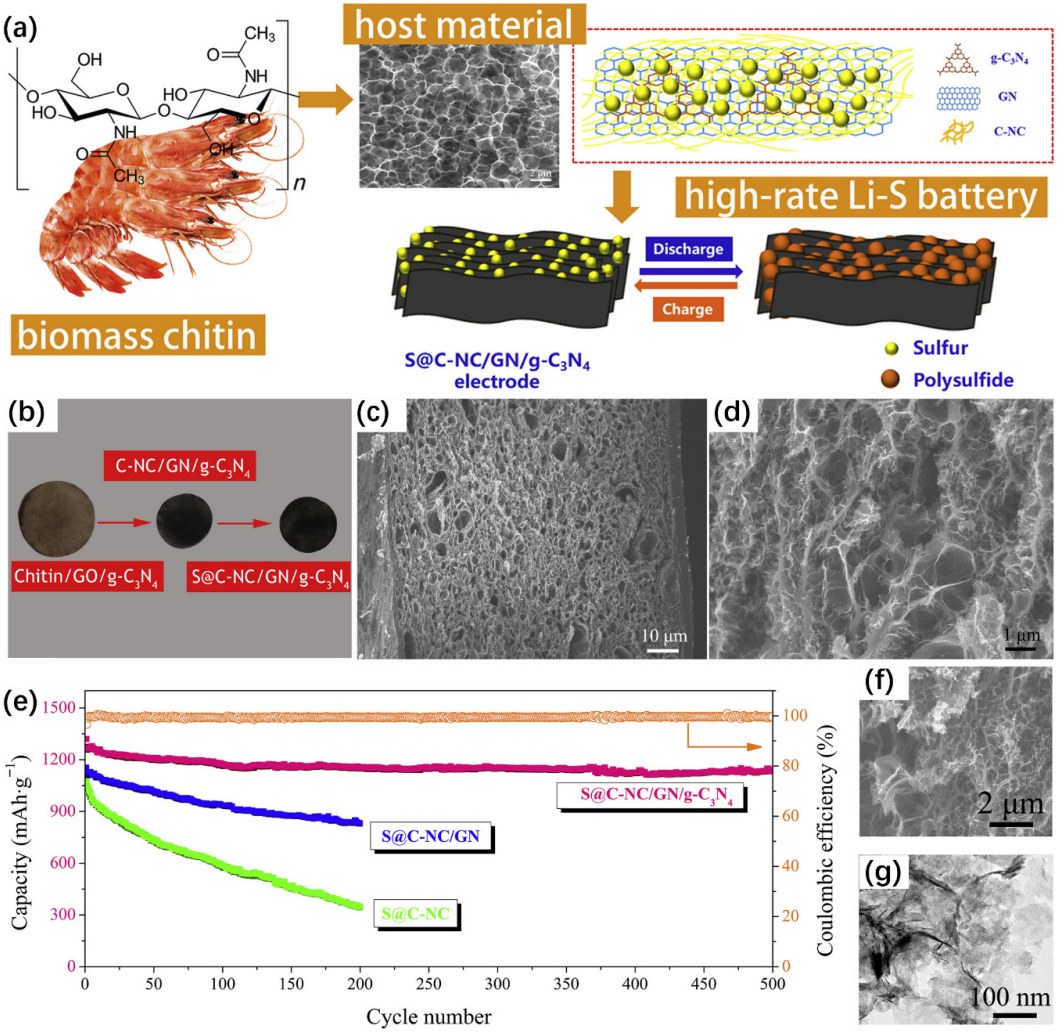

Figure 9 (a) Illustration of the synthesis process of the C-NC/GN/g-C_3N_4 hybrids. (b) Optical photos of the chitin/GO/g-C_3N_4 and C-NC/GN/g-C_3N_4 hybrids sheets, as well as the fabricated S@C-NC/GN/g-C_3N_4 electrode. (c) and (d) Cross-section SEM images of the S@C-NC/GN/g-C_3N_4 electrode under different magnification. (e) Cycling performances of the S@C-NC, S@C-NC/GN and S@C-NC/GN/g-C_3N_4 electrodes at 0.5 C, and the corresponding Coulombic efficiency of the S@CNC/ GN/g-C_3N_4 electrodes; (f) SEM and (g) TEM images of the S@C-NC/GN/g-C_3N_4 electrode after 200 cycles. Reproduced with permission from Ref. [89], © Elsevier Ltd. 2020.

resulting from the different energy bands of g-C_3N_4 and n-doped porous carbon. In another study by Song et al. [92] lightweight g-C_3N_4/carbon hybrid cages were designed and prepared as sulfur hosts using NaCl and nano-manganese compounds (MnO and $MnCN_2$) as templates through an aerosol pyrolysis pathway. The NaCl template allowed for the formation of cage cavities, designed to increase the sulfur load content. The electrochemical evaluation demonstrated that the core-shell structure of S@ g-C_3N_4/carbon cathode, with the versatile and chemical properties of the g-C_3N_4/carbon host cage structure, exhibits good cycle capacity and stability. The first cycle discharge capacity reached 1517 mAh·g^{-1} at 0.2 C and 1240 mAh·g^{-1} at 1 C, effectively utilizing the carried sulfur. Subsequently, 400 charge-discharge cycles were performed at 1 C (starting from the second cycle), with a capacity attenuation rate of each cycle at 0.09%. These lightweight, conductive, and polar g-C_3N_4/carbon cages are suitable carriers for loading sulfur as cathodes in high-performance Li-S batteries.

The use of porous carbon materials in Li-S batteries has shown promising results in addressing the challenges associated with the "shuttle effect" and improving the cycle life of the batteries. Gong et al. [93] developed a 3D lightweight porous g-C_3N_4 graphene oxide (PCN@rGO) network to overcome these challenges. The PCN@rGO cathode demonstrated chemical solid adsorption of polysulfides, fast electron and mass transfer paths, and high reversible capacity. It provided specific capacities ranging from 1205 to 483 mAh·g^{-1} at different rates, with a low-capacity attenuation rate of 0.048 after 800 cycles at 0.5 C. Similarly, Wu et al. [94] utilized porous g-C_3N_4 to synthesize nanotubes (PCNNT) through a self-template method, which served as efficient sulfur host materials. The one-dimensional PCNNTs exhibit a high specific surface area, enabling a sulfur loading rate of 74.7 wt.%. The Li-S battery with PCNNTs/S composite as the cathode demonstrates excellent cycle stability, with a capacity decrease of only 0.021% after 800 cycles at 0.5 C. The tubular structure of PCNNTs helped alleviate volume expansion during charge-discharge cycles, while the high nitrogen content enhanced the adsorption capacity of carbon nitride for lithium polysulfides. These synergistic effects contributed to the outstanding cycle stability and rate performance of the PCNNTs/S composite electrodes. Overall, utilizing lightweight porous g-C_3N_4 materials as sulfur hosts in Li-S batteries offers a promising solution for achieving high energy density and long cycle life.

In general, in the application of g-C_3N_4 in Li-S battery, defect engineering, heteroatom doping and composite materials further optimize the performance of Li-S battery, the various modification strategies of g-C_3N_4 are detailed in the Fig. 10. Each of the three

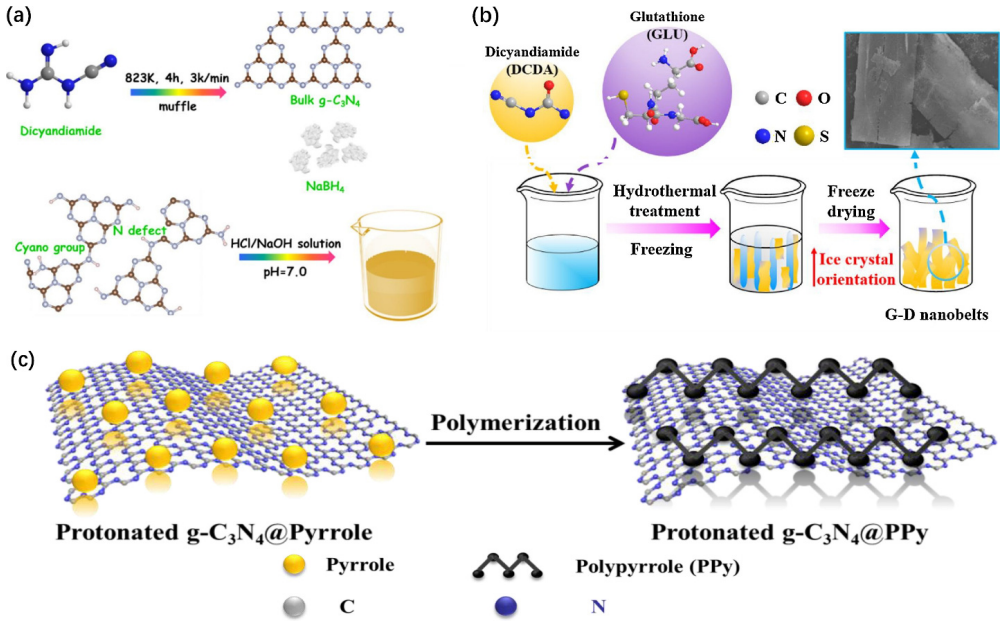

Figure 10 Various modification strategies of g-C_3N_4 in Li-S battery applications. (a) Defect Engineering. Reproduced with permission from Ref. [95], © Elsevier B.V. 2021. (b) Heteroatom doping. Reproduced with permission from Ref. [96], © American Chemical Society 2020. (c) Porous carbon material coating. Reproduced with permission from Ref. [97], © Elsevier Ltd. 2017.

methods has its own unique characteristics, and there is no absolute "best". The specific choice depends on the application requirements and performance requirements. Now a further comparison is made between these three methods. Defect engineering is to improve the catalytic activity of g-C_3N_4 and the adsorption capacity of sulfur by introducing defects [95], so as to improve the performance of the battery (Fig. 10(a)). However, defect engineering may reduce the structural stability and conductivity of the material, thus affecting the cycle life and energy density of the battery. Heteroatom doping regulates the electronic structure and catalytic performance of g-C_3N_4 by doping heteroatoms (Fig. 10(b)), so as to improve the energy density and cycle stability of the battery [96]. However, heteroatom doping may affect the structural integrity and stability of the materials and reduce the cycle life of the battery. By compounding with other materials, the composite can improve the conductivity, structural stability and catalytic performance of g-C_3N_4 (Fig. 10(c)), thus improving the performance of the battery [97]. However, composite materials may increase the weight and cost of the battery, and affect the energy density and cycle life of the battery. To sum up, these three methods have their own advantages and disadvantages, and need to be selected and optimized according to specific application requirements and performance requirements. In practical applications, a variety of methods can be combined to achieve the best performance and cost-effectiveness.

5 Conclusions summary and prospect

As a material with a distinctive structure and properties, g-C_3N_4 demonstrates substantial advantages in catalysis, polarization inhibition, electron conductivity, and sulfurization resistance, thereby addressing critical deficiencies of Li-S batteries. In this review, the advancements in research on g-C_3N_4 materials in Li-S batteries are summarized, with an emphasis on composite design, heteroatom inclusion, and defect engineering. It emphasizes the innovation and comprehensive comprehension of g-C_3N_4 materials and suggests future design strategies for their use in Li-S batteries.

5.1 Structure optimization and design

When it comes to improving the overall performance of Li-S batteries, the optimization and design of g-C_3N_4 materials are two of the most important factors. As a result of raising the surface area, building multi-stage pore structures, and establishing controlled conductive channels, it is possible to considerably improve the sulfur load capacity. The increased use of the sulfur cathode is made possible as a result of these enhancements, which give more active reaction sites within the system. In addition, the improvement of the microstructure of g-C_3N_4 makes it possible for sulfur species to be dispersed and contained more effectively, which guarantees a more effective usage of active materials throughout the charge-discharge cycles of the battery.

Furthermore, in order to efficiently trap polysulfides and limit their movement within the battery, it is essential to build customized pore architectures in order to address the shuttle effect, which is a significant difficulty in Li-S batteries. Because of this, not only does the cycle stability of the battery improve, but the overall efficiency of the gadget as well as its longevity also receives an improvement. Therefore, the strategic enhancement of the g-C_3N_4 structure is a vital approach to unlocking the full potential of Li-S batteries, which will make them more viable for practical applications in the field of energy storage.

5.2 Interface engineering

For the purpose of greatly enhancing the performance of Li-S batteries, it is essential to enhance the interaction between g-C_3N_4 materials, electrolytes, and sulfides. By reducing the impedance of the interface, which in turn improves the cycle stability and overall electrochemical performance of the battery, advanced interface engineering strategies are essential. These strategies include adjusting the composition of the electrolyte and integrating functional interface layers.

By painstakingly designing functional interface layers, it is possible to improve the adhesion between g-C_3N_4 and sulfur species. This not only makes charge transfer across the interface more efficient, but it also reduces the production of passivation

layers, which can lead to a decline in battery performance over time. The presence of these layers is essential in creating a constant and efficient reaction environment, which ultimately results in a battery that behaves in a manner that is more stable and predictable during cycling.

Additionally, adjusting the electrolyte composition is necessary for maintaining a stable SEI, which is vital for the long-term stability and performance of the battery. A SEI that has been thoughtfully developed not only safeguards the materials that make up the electrodes, but it also inhibits unfavorable side reactions that could result in capacity fading. It is possible to obtain optimal performance by fine-tuning the interface interactions within the battery by carefully balancing these aspects. This will result in Li-S batteries being more reliable and efficient for a wide variety of applications.

5.3 Advanced conductive agents and reaction mechanisms

A critical strategy for improving the performance of g-C_3N_4-based Li-S batteries is the investigation of novel conductive agents and carrier materials. The efficiency of electron transport can be considerably enhanced, as well as the entrapment of sulfur species, by incorporating materials such as two-dimensional structures, porous architectures, or other innovative designs. For example, the combination of graphene or carbon nanotubes with g-C_3N_4 generates hybrid materials that exhibit exceptional mechanical stability and conductivity, resulting in a substantial enhancement in the overall performance of batteries.

In addition to enhancing electron movement, these composite structures also reinforce the mechanical integrity of the battery, thereby enabling more consistent and reliable operation over extended cycles. The synergistic effect of the combination of g-C_3N_4 and these advanced materials optimizes both the chemical and physical properties necessary for high-performance energy storage.

Additionally, it is imperative to possess a comprehensive comprehension of the reaction mechanisms that involve sulfides in Li-S batteries in order to effectively optimize these materials. Researchers can acquire valuable insights into the formation of dendrites, dissolution processes, and reaction kinetics by utilizing advanced characterization techniques and computational simulations-factors that significantly impact battery life and stability. These insights are essential for the development of strategies to resolve issues such as rapid capacity fade and poor cycling stability, as well as for the guidance of the design of more effective g-C_3N_4-based materials. The potential of g-C_3N_4 in Li-S batteries can be fully realized through this integrated approach, thereby facilitating the development of more efficient and durable energy storage solutions.

Acknowledgements

This work was financially supported by the National Natural Science Foundation of China (No. 52271211), China; the science and technology innovation Program of Hunan Province (2023RC3185), China; HORIZON-Marie Skłodowska-Curie Actions-2021-PF (No. 101065098), European Union.

Declaration of conflicting interests

The authors declare no conflicting interests regarding the content of this article.

Data availability

All data needed to support the conclusions in the paper are presented in the manuscript and/or the Supplementary Materials. Additional data related to this paper may be requested from the corresponding author upon request.

References

[1] Liu, J.; Zhou, Y. H.; Yan, T. Y.; Gao, X. P. Perspectives of high-performance Li–S battery electrolytes. *Adv. Funct. Mater.* **2024**, *34*, 2309625.

[2] Zhang, H.; Zhang, M. T.; Liu, R. Y.; He, T. F.; Xiang, L. X.; Wu, X. R.; Piao, Z. H.; Jia, Y. Y.; Zhang, C. Y.; Li, H. et al. Fe_3O_4-doped mesoporous carbon cathode with a plumber's nightmare structure for high-performance Li–S batteries. *Nat. Commun.* **2024**, *15*, 5451.

[3] Xu, X. L.; Wang, S. J.; Wang, H.; Xu, B.; Hu, C.; Jin, Y.; Liu, J. B.; Yan, H. The suppression of lithium dendrite growth in lithium sulfur batteries: A review. *J. Energy Storage* **2017**, *13*, 387–400.

[4] Luo, J.; Li, H. Y.; Yu, G.; Xu, W. Y.; Yin, H.; Hou, Z. H. Multifunctional sandwich-structured double-carbon-layer modified SnS nanotubes with high capacity and stability for Li-ion batteries. *Mater. Adv.* **2022**, *3*, 3631–3641.

[5] Chen, Y. Z.; Zou, K. Y.; Dai, X.; Bai, H. H.; Zhang, S. L.; Zhou, T. F.; Li, C. X.; Liu, Y. N.; Pang, W. K.; Guo, Z. P. Polysulfide filter and dendrite inhibitor: Highly graphitized wood framework inhibits polysulfide shuttle and lithium dendrites in Li–S batteries. *Adv. Funct. Mater.* **2021**, *31*, 2102458.

[6] Li, H. Y.; Luo, J.; Han, D. Y.; Liu, A.; Zhou, M.; Huang, J. L.; Zhu, Y. C.; Hou, Z. H.; Yin, H. Layer-by-layer hetero-carbon modifying ZnS nanocubes anode with improved long-term life for sodium-ion batteries. *Ceram. Int.* **2023**, *49*, 18421–18431.

[7] Waluś, S.; Offer, G.; Hunt, I.; Patel, Y.; Stockley, T.; Williams, J.; Purkayastha, R. Volumetric expansion of lithium-sulfur cell during operation-fundamental insight into applicable characteristics. *Energy Storage Mater.* **2018**, *10*, 233–245.

[8] Han, D. Y.; Yu, G.; Liu, A.; Li, G. Y.; Wang, W.; He, B. H.; Hou, Z. H.; Yin, H. Soft-template-assisted synthesis of N-doping layered CoS_2 nanoparticles as an advanced anode for sodium-ion batteries. *Carbon Lett.* **2023**, *33*, 1839–1846.

[9] Ji, X. L.; Lee, K. T.; Nazar, L. F. A highly ordered nanostructured carbon-sulphur cathode for lithium-sulphur batteries. *Nat. Mater.* **2009**, *8*, 500–506.

[10] Zhang, H. H.; He, H. N.; Luan, J. Y.; Huang, X. B.; Tang, Y. G.; Wang, H. Y. Adjusting the yolk-shell structure of carbon spheres to boost the capacitive K^+ storage ability. *J. Mater. Chem. A* **2018**, *6*, 23318–23325.

[11] Wang, H. L.; Yang, Y.; Liang, Y. Y.; Robinson, J. T.; Li, Y. G.; Jackson, A.; Cui, Y.; Dai, H. J. Graphene-wrapped sulfur particles as a rechargeable lithium-sulfur battery cathode material with high capacity and cycling stability. *Nano Lett.* **2011**, *11*, 2644–2647.

[12] Zheng, G. Y.; Yang, Y.; Cha, J. J.; Hong, S. S.; Cui, Y. Hollow carbon nanofiber-encapsulated sulfur cathodes for high specific capacity rechargeable lithium batteries. *Nano Lett.* **2011**, *11*, 4462–4467.

[13] Zhou, G. M.; Paek, E.; Hwang, G. S.; Manthiram, A. High-performance lithium-sulfur batteries with a self-supported, 3D Li_2S-doped graphene aerogel cathodes. *Adv. Energy Mater.* **2016**, *6*, 1501355.

[14] Luo, J.; Xiang, S. L.; Han, D. Y.; Liu, A.; Cunha, J.; Li, G. Y.; Hou, Z. H.; Yin, H. Interface engineering of Co_9S_8/SnS heterostructure as a high-performance anode for lithium/sodium-ion batteries. *Rare Met.* **2024**, *43*, 612–623.

[15] Yin, H.; Li, H. Y.; Zhao, H.; Gan, Z. S.; Hou, Z. H.; Li, C.; Zhu, M. Q. SnSe nanoplates swallowed in carbon nanofibers as the self-standing anode for lithium-ion and sodium batteries with enhanced performance. *Int. J. Hydrogen Energy* **2023**, *48*, 4789–4799.

[16] Guo, T. Q.; Zhou, Y. R.; Wang, Z. C.; Cunha, J.; Alves, C.; Ferreira,

P.; Hou, Z. H.; Yin, H. Indium nitride nanowires: Low redox potential anodes for lithium-ion batteries. *Adv. Sci.* **2024**, *11*, 2310166.
[17] He, B. H.; Cunha, J.; Hou, Z. H.; Li, G. Y.; Yin, H. 3D hierarchical self-supporting Bi_2Se_3-based anode for high-performance lithium/sodium-ion batteries. *J. Colloid Interface Sci.* **2023**, *650*, 857–864.
[18] Yin, H.; Deng, Y. Q.; He, Z.; Xu, W. Y.; Hou, Z. H.; He, B. H.; Çaha, İ.; Cunha, J.; Karimi, M.; Yu, Z. P. Strain engineering of Co_{SA}–N–C catalyst toward enhancing the oxygen reduction reaction activity. *J. Colloid Interface Sci.* **2025**, *678*, 447–457.
[19] Yin, H.; Yu, Z. P. Hexavalent iridium catalyst enhances efficiency of hydrogen production. *Chin. J. Struc. Chem.*, in press, DOI: 10.1016/j.cjsc.2024.100382.
[20] Yuan, C. Z.; Huang, S. Y.; Zhao, H. R. Li, J.; Zhang, L. L.; Weng, Y.; Cheang, T. Y.; Yin, H.; Zhang, X. M.; Ye, S. F. Vacancy defect tuning of electronic structures of transition metal (hydr)oxide-based electrocatalysts for enhanced oxygen evolution. *Energy Adv.* **2023**, *2*, 73–85.
[21] Xiao, X. Q.; Guo, F. J.; Mi, H. Y.; Chang, X. Q.; Yin, H.; Ji, C. C.; Qiu, J. S. Controlling dendrite growth with xylan-enhanced hydroxyl-rich hydrogel electrolyte for efficient Zn-ion energy storage. *ACS Sustain. Chem. Eng.* **2024**, *12*, 470–479.
[22] Yin, H.; Li, H. Y.; Yu, X. X.; Cao, M. L. Design of Sb_2Te_3 nanoblades serialized by Te nanowires for a low-temperature near-infrared photodetector. *Front. Chem.* **2022**, *10*, 1060523.
[23] Shi, Z. X.; Thomas, S.; Tian, Z. N.; Guo, D.; Zhao, Z. M.; Wang, Y. Z.; Li, S.; Wehbe, N.; Emwas, A. H.; Bakr, O. M. et al. A tailored highly solvating electrolyte toward ultra lean-electrolyte Li–S batteries. *Nano Res. Energy*, in press, DOI: 10.26599/NRE.2024.9120126.
[24] Wang, B. L.; Ye, L.; Yin, H.; Yu, X. X. Ferroelectrically tuned tunneling photodetector based on graphene/h-BN/In_2Se_3 heterojunction. *Opt. Mater.* **2024**, *150*, 115264.
[25] Zhao, H. R.; Yuan, C. Z.; Li, C. H.; Zhao, W. K.; Wu, F. L.; Xin, L.; Yin, H.; Ye, S. F.; Zhang, X. M.; Chen, Y. F. Structure deformation of Ni–Fe–Se enables efficient oxygen evolution via RE atoms doping. *Rare Met.*, in press, DOI: 10.1007/s12598-024-02900-9.
[26] Weng, G. M.; Xie, Y.; Wang, H.; Karpovich, C.; Lipton, J.; Zhu, J. Q.; Kong, J.; Pfefferle, L. D.; Taylor, A. D. A promising carbon/g-C_3N_4 composite negative electrode for a long-life sodium-ion battery. *Angew. Chem.* **2019**, *131*, 13865–13871.
[27] Desalegn, B. Z.; Jadhav, H. S.; Seo, J. G. Highly efficient g-C_3N_4 nanorods with dual active sites as an electrocatalyst for the oxygen evolution reaction. *ChemCatChem* **2019**, *11*, 2870–2878.
[28] Liu, Z. X.; Zhu, Y. P.; El-Demellawi, J. K.; Velusamy, D. B.; El-Zohry, A. M.; Bakr, O. M.; Mohammed, O. F.; Alshareef, H. N. Metal halide perovskite and phosphorus doped g-C_3N_4 bulk heterojunctions for air-stable photodetectors. *ACS Energy Lett.* **2019**, *4*, 2315–2322.
[29] Zhang, Y.; Sun, S.; Wu, Y. Y.; Chen, F. F. Emerging roles of graphitic carbon nitride-based materials in biomedical applications. *ACS Biomater. Sci. Eng.* **2024**, *10*, 4645–4661.
[30] Chen, Z. X.; Zheng, B. Y.; Li, X. X.; Fu, M. L.; Xie, S. G.; Deng, C.; Hu, Y. H. Progress in the preparation of nanomaterials employing template method. *Chem. Ind. Eng. Prog.* **2010**, *29*, 94–99.
[31] Wang, Z. H.; Jin, B. J.; Peng, J.; Su, W.; Zhang, K.; Hu, X.; Wang, G. N.; Park, J. H. Engineered polymeric carbon nitride additive for energy storage materials: A review. *Adv. Funct. Mater.* **2021**, *31*, 2102300.
[32] Li, Y.; Liu, Z.; Li, Z.; Wang, Q. Renewable biomass-derived carbon-supported g-C_3N_4 doped with Ag for enhanced photocatalytic reduction of CO_2. *J. Colloid Interface Sci.* **2022**, *606*, 1311–1321.
[33] Kumar, A.; Kashyap, S.; Sharma, M.; Krishnan, V. Tuning the surface and optical properties of graphitic carbon nitride by incorporation of alkali metals (Na, K, Cs and Rb): Effect on photocatalytic removal of organic pollutants. *Chemosphere* **2022**, *287*, 131988.
[34] Liu, Z. Q.; Zhang, W. T.; Yin, H.; Guo, F. J.; Mi, H. Y.; Liang, Y. X.; Qiu, J. S. Gradient solid electrolyte interphase exerted by robust hydrogel electrolyte-Zn interface and alkaloid additive enables reversible and durable Zn anodes. *Chem. Eng. J.* **2024**, *497*, 154787.
[35] Guo, S. E.; Tang, Y. Q.; Xie, Y.; Tian, C. G.; Feng, Q. M.; Zhou, W.; Jiang, B. J. P-doped tubular g-C_3N_4 with surface carbon defects: Universal synthesis and enhanced visible-light photocatalytic hydrogen production. *Appl. Catal. B Environ.* **2017**, *218*, 664–671.
[36] Chen, F.; Yang, H.; Wang, X. F.; Yu, H. G. Facile synthesis and enhanced photocatalytic H_2-evolution performance of NiS_2-modified g-C_3N_4 photocatalysts. *Chin. J. Catal.* **2017**, *38*, 296–304.
[37] Li, Y.; Feng, X. H.; Lu, Z. X.; Yin, H.; Liu, F.; Xiang, Q. J. Enhanced photocatalytic H_2-production activity of C-dots modified g-C_3N_4/TiO_2 nanosheets composites. *J. Colloid Interface Sci.* **2018**, *513*, 866–876.
[38] Zhou, X.; Liu, T. T.; Zhao, G. F.; Yang, X. F.; Guo, H. Cooperative catalytic interface accelerates redox kinetics of sulfur species for high-performance Li–S batteries. *Energy Storage Mater.* **2021**, *40*, 139–149.
[39] Zhou, M.; Zhou, X. T.; Yang, Y.; Yin, H.; Lei, Y. P.; Liang, S. Q.; Fang, G. Z. Issues and optimization strategies of binders for aqueous zinc metal batteries. *Chem. Eng. J.* **2024**, *497*, 154916.
[40] Sun, X. H.; An, X. H.; Zhang, S.; Li, Z. T.; Zhang, J.; Wu, W. T.; Wu, M. B. Physical vapor deposition (PVD): A method to fabricate modified g-C_3N_4 sheets. *New J. Chem.* **2019**, *43*, 6683–6687.
[41] Liu, R.; Bie, Y. C.; Qiao, Y. J.; Liu, T.; Song, Y. J. Design of g-C_3N_4/TiO_2 nanotubes heterojunction for enhanced organic pollutants degradation in waste water. *Mater. Lett.* **2019**, *251*, 126–130.
[42] Wang, Y. G.; Wang, F.; Zuo, Y. H.; Zhang, X. D.; Cui, L. F. Simple synthesis of ordered cubic mesoporous graphitic carbon nitride by chemical vapor deposition method using melamine. *Mater. Lett.* **2014**, *136*, 271–273.
[43] Cao, M. Y.; Wang, K.; Tudela, I.; Fan, X. F. Improve photocatalytic performance of g-C_3N_4 through balancing the interstitial and substitutional chlorine doping. *Appl. Surf. Sci.* **2021**, *536*, 147784.
[44] Zhang, B.; Shi, H. X.; Yan, Y. J.; Liu, C. Q.; Hu, X. Y.; Liu, E. Z.; Fan, J. A novel S-scheme 1D/2D Bi_2S_3/g-C_3N_4 heterojunctions with enhanced H_2 evolution activity. *Colloids Surf. A: Physicochem. Eng. Asp.* **2021**, *608*, 125598.
[45] Yan, S. C.; Li, Z. S.; Zou, Z. G. Photodegradation performance of g-C_3N_4 fabricated by directly heating melamine. *Langmuir* **2009**, *25*, 10397–10401.
[46] Wang, Y.; Wang, X. C.; Antonietti, M.; Zhang, Y. J. Facile one-pot synthesis of nanoporous carbon nitride solids by using soft templates. *ChemSusChem* **2010**, *3*, 435–439.
[47] Ji, H. H.; Chang, F.; Hu, X.; F.; Qin, W.; Shen, J. W. Photocatalytic degradation of 2,4,6-trichlorophenol over g-C_3N_4 under visible light irradiation. *Chem. Eng. J.* **2013**, *218*, 183–190.
[48] Zhang, Y. W.; Liu, J. H.; Wu, G.; Chen, W. Porous graphitic carbon nitride synthesized via direct polymerization of urea for efficient sunlight-driven photocatalytic hydrogen production. *Nanoscale* **2012**, *4*, 5300–5303.
[49] Zhang, G. G.; Zhang, J. S.; Zhang, M. W.; Wang, X. C. Polycondensation of thiourea into carbon nitride semiconductors as visible light photocatalysts. *J. Mater. Chem.* **2012**, *22*, 8083–8091.
[50] Jia, Z. Y.; Zhang, H. Z.; Yu, Y.; Chen, Y. Q.; Yan, J. W.; Li, X. F.; Zhang, H. M. Trithiocyanuric acid derived g-C_3N_4 for anchoring the polysulfide in Li–S batteries application. *J. Energy Chem.* **2020**, *43*, 71–77.
[51] Huangfu, Y. G.; Zheng, T. T.; Zhang, K.; She, X. J.; Xu, H.; Fang, Z.; Xie, K. Y. Facile fabrication of permselective g-C_3N_4 separator for improved lithium-sulfur batteries. *Electrochim. Acta* **2018**, *272*, 60–67.
[52] Luo, M.; Bai, Y.; Sun, R.; Wang, Z. H.; Sun, W.; Lin, P.; Dai, X.; Sun, K. N. Enhanced performance of lithium-sulfur batteries with Co-doped g-C_3N_4 nanosheet-based separator. *Ind. Eng. Chem. Res.* **2021**, *60*, 1231–1240.
[53] Li, D. S.; Liu, J.; Wang, W. J.; Li, S. M.; Yang, G. L.; Wang, P.;

Zhu, K. X.; Li, Z. J. Synthesis of porous N deficient graphitic carbon nitride and utilization in lithium-sulfur battery. *Appl. Surf. Sci.* **2021**, *569*, 151058.
[54] Ma, H.; Song, C. L.; Liu, N.; Zhao, Y.; Bakenov, Z. Nitrogen-deficient graphitic carbon nitride/carbon nanotube as polysulfide barrier of high-performance lithium-sulfur batteries. *Chemelectrochem* **2020**, *7*, 4906–4912.
[55] Zhang, S. S. Heteroatom-doped carbons: Synthesis, chemistry and application in lithium/sulphur batteries. *Inorg. Chem. Front.* **2015**, *2*, 1059–1069.
[56] Lu, C.; Chen, Y.; Yang, Y.; Chen, X. Single-atom catalytic materials for lean-electrolyte ultrastable lithium-sulfur batteries. *Nano Lett.* **2020**, *20*, 5522–5530.
[57] Chen, M. F.; Zhao, X. M.; Li, Y. F.; Zeng, P.; Liu, H.; Yu, H.; Wu, M.; Li, Z. H.; Shao, D. S.; Miao, C. Q. et al. Kinetically elevated redox conversion of polysulfides of lithium-sulfur battery using a separator modified with transition metals coordinated g-C_3N_4 with carbon-conjugated. *Chem. Eng. J.* **2020**, *385*, 123905.
[58] Zhang, W. Q.; Chen, M. F.; Luo, Y. X.; He, Y. Q.; Liu, S. S.; Ye, Y. J.; Wang, M. Q.; Chen, Y.; Zhu, K.; Shu, H. B. et al. Utilizing 2D layered structure Cu-g-C_3N_4 electrocatalyst for optimizing polysulfide conversion in wide-temperature Li–S batteries. *Chem. Eng. J.* **2024**, *486*, 150411.
[59] Sun, Y. J.; Huang, W. Z.; Li, J. H.; Pan, J. J.; Nan, H. X.; Dong, H. F.; Shi, K. X.; Liu, Q. B. Designing polysulfides adsorption-conversion on g-C_3N_4-based separator via doping heteroatoms boron and phosphorus toward high-performance lithium-sulfur batteries. *AIChE J.* **2023**, *69*, e17940.
[60] Ding, L.; Lu, Q. Q.; Permana, A. D. C.; Oswald, S.; Hantusch, M.; Nielsch, K.; Mikhailova, D. Oxygen-doped carbon nitride tubes for highly stable lithium-sulfur batteries. *Energy Technol.* **2021**, *9*, 2001057.
[61] Chen, Y. Y.; Wu, Y.; Li, L.; Liao, Y.; Luo, S.; Wu, Y. Q.; Qing, Y. Polysulfides manipulation: Constructing g-C_3N_4 networks encapsulated into natural wood fibers for high-performance lithium-sulfur batteries. *Chem. Eng. J.* **2023**, *461*, 141988.
[62] Do, V.; Deepika; Kim, M. S.; Lee, K. R.; Cho, W. I. Carbon nitride phosphorus as an effective lithium polysulfide adsorbent for lithium-sulfur batteries. *ACS Appl. Mater. Interfaces* **2019**, *11*, 11431–11441.
[63] Xu, G.; Li, L.; Li, M. C.; Xi, C. P.; Yan, J. W.; Li, R.; Chao, Y.; Yang, C. K.; Yu, Y. Suitable polysulfides adsorption and conversion on $MoSe_2$@g-C_3N_4 interlayer for advanced lithium-sulfur batteries. *Appl. Surf. Sci.* **2022**, *604*, 154556.
[64] Wen, K. N.; Huang, L.; Qu, L. T.; Deng, T.; Men, X. L.; Chen, L. P.; Wang, J. g-C_3N_4/MoO_3 composite with optimized crystal face: A synergistic adsorption-catalysis for boosting cathode performance of lithium-sulfur batteries. *J. Colloid Interface Sci.* **2023**, *649*, 890–899.
[65] Wang, Y.; Yang, L. W.; Chen, Y. X.; Li, Q.; Chen, C. T.; Zhong, B. H.; Guo, X. D.; Wu, Z. G.; Wang, G. K. Novel bifunctional separator with a self-assembled FeOOH/coated g-C_3N_4/KB bilayer in lithium-sulfur batteries. *ACS Appl. Mater. Interfaces* **2020**, *12*, 57859–57869.
[66] Dong, L. L.; Jiang, W.; Pan, K. F.; Zhang, L. P. Rational design of TiO_2@g-C_3N_4/CNT composite separator for high performance lithium-sulfur batteries to promote the redox kinetics of polysulfide. *Nanomaterials* (*Basel*) **2023**, *13*, 3084.
[67] Majumder, S.; Shao, M. H.; Deng, Y. F.; Chen, G. H. Ultrathin sheets of MoS_2/g-C_3N_4 composite as a good hosting material of sulfur for lithium-sulfur batteries. *J. Power Sources* **2019**, *431*, 93–104.
[68] Xu, J.; Xu, Y. Y.; Tang, G. G.; Tang, H.; Jiang, H. B. The novel g-C_3N_4/MoS_2/ZnS ternary nanocomposite with enhanced lithium storage properties. *Appl. Surf. Sci.* **2019**, *492*, 37–44.
[69] Li, Y. A.; Deng, Y. R.; Yang, J. L.; Tang, W. H.; Ge, B.; Liu, R. P. Bidirectional catalyst with robust lithiophilicity and sulfiphilicity for advanced lithium-sulfur battery. *Adv. Funct. Mater.* **2023**, *33*, 2302267.
[70] Liu, H. Y.; Li, X. Y.; Ma, L. M.; Sun, F.; Yue, B.; Ma, Q. L.; Wang, J. X.; Liu, G. X.; Yu, H.; Yu, W. S. et al. *In-situ* growth of g-C_3N_4 nanosheets on Nb_2O_5 nanofibers for enhanced performance in photocatalysis and lithium-sulfur battery. *Colloids Surf. A: Physicochem. Eng. Asp.* **2023**, *670*, 131572.
[71] Liu, X. Y.; Wang, S. X.; Duan, H. H.; Deng, Y. F.; Chen, G. H. A thin and multifunctional CoS@g-C_3N_4/Ketjen black interlayer deposited on polypropylene separator for boosting the performance of lithium-sulfur batteries. *J. Colloid Interface Sci.* **2022**, *608*, 470–481.
[72] Abd-Alkuder Salman, E.; Abaid Samawi, K.; Fawzi Nassar, M.; Abdulkareem-Alsultan, G.; Abdulmalek, E. 3D hollow spheres comprising MXene/g-C_3N_4 heterostructre for efficient polysulfide adsorption and conversion in high-performance Li–S batteries. *J. Electroanal. Chem.* **2023**, *945*, 117629.
[73] Yin, H.; Shen, W. Q.; Qu, H. Q.; Li, C.; Zhu, M. Q. Boosted charge transfer and Na-ion diffusion in cooling-fins-like Sb_2Te_3-Te nano-heterostructure for long cycle life and high rate capability anode. *Nano Energy* **2020**, *70*, 104468.
[74] Yin, H.; Qu, H. Q.; Liu, Z. T.; Jiang, R. Z.; Li, C.; Zhu, M. Q. Long cycle life and high rate capability of three dimensional $CoSe_2$ grain-attached carbon nanofibers for flexible sodium-ion batteries. *Nano Energy* **2019**, *58*, 715–723.
[75] Kang, Y.; Wang, S.; Zhu, S. Q.; Gao, H. X.; Hui, K. S.; Yuan, C. Z.; Yin, H.; Bin, F.; Wu, X. L.; Mai, W. J. et al. Iron-modulated nickel cobalt phosphide embedded in carbon to boost power density of hybrid sodium-air battery. *Appl. Catal. B Environ.* **2021**, *285*, 119786.
[76] Yu, X. X.; Wang, L.; Yin, H. Hierarchical heterojunction structures based-on layered Sb_2Te_3 nanoplate@rGO for extended long-term life and high-rate capability of sodium batteries. *Appl. Mater. Today* **2019**, *15*, 582–589.
[77] Wang, W. B.; Dong, W.; Hong, X. D.; Liu, Y. H.; Yang, S. B. Preparation of g-C_3N_4/CNTs composite by dissolution-precipitation method as sulfur host for high-performance lithium-sulfur batteries. *Mater. Chem. Phys.* **2022**, *283*, 126014.
[78] Wang, X. L.; Li, G. R.; Li, M. J.; Liu, R. P.; Li, H. B.; Li, T. Y.; Sun, M. Z.; Deng, Y. R.; Feng, M.; Chen, Z. W. Reinforced polysulfide barrier by g-C_3N_4/CNT composite towards superior lithium-sulfur batteries. *J. Energy Chem.* **2021**, *53*, 234–240.
[79] Zhang, H. J.; Liu, Q. Z.; Ruan, S. J.; Ma, C.; Jia, X. F.; Qiao, W. M.; Ling, L. C.; Wang, J. T. *In-situ* construction of g-C_3N_4/carbon heterostructure on graphene nanosheet: An efficient polysulfide barrier for advanced lithium-sulfur batteries. *Appl. Surf. Sci.* **2022**, *578*, 152022.
[80] Ye, H. L.; Li, Y. G. Towards practical lean-electrolyte Li–S batteries: Highly solvating electrolytes or sparingly solvating electrolytes. *Nano Res. Energy* **2022**, *1*, e9120012.
[81] Yin, H.; Han, D. Y.; Yu, X. X.; Cao, M. L.; Hou, Z. H.; Li, C.; Zhu, M. Q. Recent advances in electrospun metal chalcogenide anodes for lithium-ion and sodium-ion batteries. *ACS Appl. Energy Mater.* **2023**, *6*, 1155–1175.
[82] Moon, S. H.; Shin, J. H.; Kim, J. H.; Jang, J. S.; Kim, S. B.; Park, Y. Y.; Lee, S. N.; Park, K. W. Polypyrrole coated g-C_3N_4/rGO/S composite as sulfur host for high stability lithium-sulfur batteries. *Mater. Chem. Phys.* **2022**, *287*, 126267.
[83] Song, J. H.; Feng, S.; Zhu, C. Z.; Lee, J. I.; Fu, S. F.; Dong, P. P.; Song, M. K.; Lin, Y. H. Tuning the structure and composition of graphite-phase polymeric carbon nitride/reduced graphene oxide composites towards enhanced lithium-sulfur batteries performance. *Electrochim. Acta* **2017**, *248*, 541–546.
[84] Wang, J. L.; Meng, Z.; Yang, W. T.; Yan, X. F.; Guo, R. N.; Han, W. Q. Facile synthesis of rGO/g-C_3N_4/CNT microspheres via an ethanol-assisted spray-drying method for high-performance lithium-sulfur batteries. *ACS Appl. Mater. Interfaces* **2019**, *11*, 819–827.
[85] Zhao, D. K.; Xu, Z. R.; Yu, X. L.; Chen, M. Z.; Wu, O. K.; Zhou, K.; Zhou, W.; Ma, L.; Wang, N. One stone two bird: Reduced oxide graphene supported g-C_3N_4 quantum dots implements efficient

capturing/catalytic polysulfides conversion and high sulfur loading for lithium-sulfur battery. *Chem. Eng. J.* **2023**, *474*, 145983.
[86] Sun, K.; Guo, P. Q.; Shang, X. N.; Fu, Y. J.; Cheng, P.; Liu, Q. M.; Weng, Q. H.; Liu, D. Q.; He, D. Y. Mesoporous boron carbon nitride/graphene modified separators as efficient polysulfides barrier for highly stable lithium-sulfur batteries. *J. Electroanal. Chem.* **2019**, *842*, 34–40.
[87] Fan, Y.; Yang, Z.; Hua, W.; X.; Liu, D.; Tao, T.; Rahman, M.; Lei, W. W.; Huang, S. M.; Chen, Y. Functionalized boron nitride nanosheets/graphene interlayer for fast and long-life lithium-sulfur batteries. *Adv. Energy Mater.* **2017**, *7*, 1602380.
[88] Deng, D. R.; Bai, C. D.; Xue, F.; Lei, J.; Xu, P.; Zheng, M. S.; Dong, Q. F. Multifunctional ion-sieve constructed by 2D materials as an interlayer for Li–S batteries. *ACS Appl. Mater. Interfaces* **2019**, *11*, 11474–11480.
[89] Wu, X. Y.; Li, S. M.; Wang, B.; Liu, J. H.; Yu, M. Free-standing 3D network-like cathode based on biomass-derived N-doped carbon/graphene/g-C_3N_4 hybrid ultrathin sheets as sulfur host for high-rate Li–S battery. *Renew. Energy* **2020**, *158*, 509–519.
[90] Qu, L.; Liu, P.; Yi, Y. K.; Wang, T.; Yang, P.; Tian, X. L.; Li, M. T.; Yang, B. L.; Dai, S. Enhanced cycling performance for lithium-sulfur batteries by a laminated 2D g-C_3N_4/graphene cathode interlayer. *ChemSusChem* **2019**, *12*, 213–223.
[91] Zou, Y. L.; Zou, H. Y.; Ao, Z. R.; Lv, Y. Y.; Chen, N. T.; Huang, Y. X. N-doped porous carbon coated g-C_3N_4/g-C_3N_4 heterojunction for polysulfide restriction and catalytic conversion towards enhanced lithium-sulfur batteries. *J. Alloys Compd.* **2023**, *940*, 168772.
[92] Song, P.; Chen, Z. L.; Chen, Y. X.; Ma, Q.; Liu, H. B. Light-weight g-C_3N_4/carbon hybrid cages as conductive and polar hosts to construct core-shell structured S@g-C_3N_4/carbon spheres with enhanced Li ion-storage performance. *Electrochim. Acta* **2020**, *363*, 137217.
[93] Gong, Y.; Fu, C. P.; Zhang, G. P.; Zhou, H. H.; Kuang, Y. F. Three-dimensional porous C_3N_4 nanosheets@reduced graphene oxide network as sulfur hosts for high performance lithium-sulfur batteries. *Electrochim. Acta* **2017**, *256*, 1–9.
[94] Wu, M. R.; Gao, M. Y.; Zhang, S. Y. Y.; Yang, R.; Chen, Y. M.; Sun, S. Q.; Xie, J. F.; Guo, X. M.; Cao, F.; Zhang, J. H. High-performance lithium-sulfur battery based on porous N-rich g-C_3N_4 nanotubes via a self-template method. *Int. J. Miner. Metall. Mater.* **2021**, *28*, 1656–1665.
[95] Qin, Y. Y.; Lu, J.; Zhao, X. Y.; Lin, X. Y.; Hao, Y.; Huo, P. W.; Meng, M. J.; Yan, Y. S. Nitrogen defect engineering and π-conjugation structure decorated g-C_3N_4 with highly enhanced visible-light photocatalytic hydrogen evolution and mechanism insight. *Chem. Eng. J.* **2021**, *425*, 131844.
[96] Wu, J. J.; Li, N.; Zhang, X. H.; Fang, H. B.; Zheng, Y. Z.; Tao, X. Heteroatoms binary-doped hierarchical porous g-C_3N_4 nanobelts for remarkably enhanced visible-light-driven hydrogen evolution. *Appl. Catal. B Environ.* **2018**, *226*, 61–70.
[97] Li, Q.; Xu, D.; Guo, J. N.; Ou, X.; Yan, F. Protonated g-C_3N_4@polypyrrole derived N-doped porous carbon for supercapacitors and oxygen electrocatalysis. *Carbon* **2017**, *124*, 599–610.

Hong Yin received his Ph.D. in electronic science and technology from Huazhong University of Science and Technology (HUST) in 2017. In 2022, he became an associate professor at Hunan Institute of Science and Technology. Since 2023, he has been a Marie Curie Research Fellow at the International Iberian Nanotechnology Laboratory (INL). His research focuses on high-performance and secure electrochemical energy storage materials and carbon fiber functional materials, particularly hybrid alkali metal-ion batteries.

Jin He is currently an undergraduate at Hunan Institute of Science and Technology. Her research interests focus on the in-depth study of solar and wind energy technologies and their innovative applications in energy conversion and storage.

Tianqi Zhang received his master's degree from the Ludong university (China) in 2020. He is currently a PhD student at the School of Chemistry and Chemical Engineering, Ocean University of China, conducting research under the supervision of Professor Meng Qiu. His research focuses on the optoelectronic properties of novel two-dimensional materials.

Zhipeng Yu received his master's degree from the South China University of Technology in 2018 and his Ph.D. degree from the University of Porto in 2022, under the supervision of Prof. Joaquim L. Faria and Prof. Lifeng Liu. He is now a Research Fellow at the International Iberian Nanotechnology Laboratory (INL) and a visiting researcher at the Songshan Lake Materials Laboratory (SLAB) in Dongguan, China. His main research interest lies in the development of advanced materials and their applications in the field of electrochemical energy conversion.